Interleukin-11 is a Marker for Both Cancer- and Inflammation-Associated Fibroblasts that Contribute to Colorectal Cancer Progression

Takashi Nishina[1, *], Yutaka Deguchi[1], Wakami Takeda[1, 2], Masato Ohtsuka[3, 4], Daisuke Ohshima[5], Soh Yamazaki[1], Mika Kawauchi[1], Eri Nakamura[6], Chiharu Nishiyama[2], Yuko Kojima[7], Satomi Adachi-Akahane[5], Mizuho Hasegawa[8], Mizuho Nakayama[9], Masanobu Oshima[9], Hideo Yagita[10], Kazutoshi Shibuya[11], Tetuo Mikami[12], Naohiro Inohara[8], Norihiro Tada[6], Hiroyasu Nakano[1, 13, 14*]

[1]Department of Biochemistry, Toho University School of Medicine, 5-21-16 Omori-Nishi, Ota-ku, Tokyo 143-8540, Japan.

[2]Laboratory of Molecular Biology and Immunology, Department of Biological Science and Technology, Faculty of Industrial Science and Technology, Tokyo University of Science, 6-3-1 Niijuku, Katsushika-ku, Tokyo, 125–8585, Japan.

[3]Department of Molecular Life Science, Division of Basic Medical Science and Molecular Medicine, School of Medicine, Tokai University, 143 Shimokasuya, Isehara,

17 Kanagawa, 259-1193, Japan.

18 [4]The Institute of Medical Sciences, Tokai University, 143 Shimokasuya, Isehara,

19 Kanagawa, 259-1193, Japan.

20 [5]Department of Physiology, Toho University School of Medicine, 5-21-16 Omori-Nishi,

21 Ota-ku, Tokyo 143-8540, Japan.

22 [6]Research Institute for Diseases of Old Age, Juntendo University School of Medicine,

23 2-1-1 Hongo, Bunkyo-ku, Tokyo 113-8421, Japan.

24 [7]Laboratory of Morphology and Image Analysis, Research Support Center, Juntendo

25 University Graduate School of Medicine, Tokyo 113-8421, Japan.

26 [8]Department of Pathology, University of Michigan Medical School, Ann Arbor, MI

27 48109, USA.

28 [9]WPI Nano Life Science Institute (WPI-Nano LSI), Division of Genetics, Cancer

29 Research Institute, Kanazawa University, Kanazawa, Ishikawa 920-1192, Japan.

30 [10]Department of Immunology, Juntendo University Graduate School of Medicine, 2-1-1

31 Hongo, Bunkyo-ku, Tokyo 113-8421, Japan.

32 [11]Department of Surgical Pathology, Toho University School of Medicine, 5-21-16

33 Omori-Nishi, Ota-ku, Tokyo 143-8540, Japan.

34 [12]Department of Pathology, Toho University School of Medicine, 5-21-16 Omori-Nishi,

35 Ota-ku, Tokyo 143-8540, Japan.

36 [13]Host Defense Research Center, Toho University School of Medicine, 5-21-16

37 Omori-Nishi, Ota-ku, Tokyo 143-8540, Japan.

38 [13]Lead contact.

39 *To whom correspondence should be addressed. E-mail:

40 takashi.nishina@med.toho-u.ac.jp or hiroyasu.nakano@med.toho-u.ac.jp

41

SUMMARY

Interleukin (IL)-11 is a member of the IL-6 family of cytokines and involved in multiple cellular responses, including tumor development. However, the origin and functions of IL-11-producing (IL-11$^+$) cells are not fully understood. To characterize IL-11$^+$ cells *in vivo*, we generated *Il11* reporter mice. IL-11$^+$ cells appeared in the colon of three murine tumor models, and a murine acute colitis model. *Il11ra1* or *Il11* deletion attenuated the development of colitis-associated colorectal cancer. IL-11$^+$ cells expressed fibroblast markers, and genes associated with cell proliferation and tissue repair. IL-11 induced STAT3 phosphorylation in colonic fibroblasts, suggesting the activation of IL-11$^+$ fibroblasts. Analysis using the human cancer database revealed that genes enriched in IL-11$^+$ fibroblasts were elevated in human colorectal cancer, and correlated with reduced disease-free survival. Together, our results suggested that tumor cells induced IL-11$^+$ fibroblasts, and that a feed-forward loop between IL-11 and IL-11$^+$ fibroblasts might contribute to tumor development.

(149 words)

58 **KEYWORDS:** cancer-associated fibroblasts, colitis, colitis-associated colorectal cancer,
59 dextran sulfate sodium, inflammation-associated fibroblasts; interleukin-11, IL-11
60 receptor, reporter mice, STAT3.
61

INTRODUCTION

Maintenance of intestinal homeostasis involves a variety of cell types, including epithelial, immune, and stromal cells[1, 2, 3]. Within the intestinal lamina propria, stromal cells include fibroblasts, α smooth muscle actin (αSMA)-positive myofibroblasts, endothelial cells, and pericytes[4, 5]. These stromal cells organize the tissue architecture, and have recently been revealed to play crucial roles in regulating immune responses, tissue repair, and tumor development[3, 4, 5]. Recent studies have focused on fibroblasts that can support tumor growth, termed cancer-associated fibroblasts (CAFs)[6, 7, 8]. In a very recent study, single-cell RNA-sequencing (scRNA-seq) was performed to analyze colon biopsies from healthy individuals and ulcerative colitis (UC) patients. The results revealed that UC patients' colon samples included a unique subset of fibroblasts, termed inflammation-associated fibroblasts (IAFs), with high expression of *IL11*, *IL24*, *IL13RA2,* and *TNFSFR11B*[9]. Another prior study demonstrated that CD10 and GPR77 might be markers of CAFs that mediate chemotherapy resistance in human cancer through IL-6 and IL-8 production[10]. Combined these findings together, stromal fibroblasts play a crucial role in the development of cancer and colitis, the full picture of

78 fibroblast function and heterogeneity remains unclear.

79 Interleukin (IL)-11 is a member of the IL-6 family, and exhibits pleiotropic
80 functions, including hematopoiesis, bone development, tissue repair, and tumor
81 development[11, 12]. The IL-11 receptor comprises IL-11Rα1, which binds IL-11, and
82 gp130, which transmits signals to the nucleus via Janus kinase (JAK) activation[13]. JAKs
83 phosphorylate STAT3, and phosphorylated STAT3 enters the nucleus where it activates
84 the transcription of various target genes associated with cell proliferation and apoptosis
85 suppression[14, 15, 16, 17]. IL-11 production is regulated by several cytokines, including
86 TGFβ, IL-1β, IL-17A, and IL-22[18, 19, 20, 21]. We previously demonstrated that IL-11
87 production is induced by reactive oxygen species (ROS) and the electrophile
88 1,2-naphthoquinone, which, in turn, promotes liver and intestine tissue repair[22, 23].
89 While IL-11 is reportedly produced in various cell types (including stromal,
90 hematopoietic, and epithelial cells) in response to different stimuli[16, 17, 24, 25], the cellular
91 sources of IL-11 *in vivo* are not fully understood.

92 Colorectal cancers exhibit increased IL-11 expression in human and mice.
93 Moreover, deletion of the *Il11ra1* gene attenuates colitis-associated colorectal cancer

(CAC) development in mice treated with azoxymethane (AOM) and dextran sulfate sodium (DSS), or in adenomatous polyps of mice harboring mutation of the *Adenomatous polyposis coli (Apc)* gene ($Apc^{Min/+}$)[17]. On the other hand, *IL11* gene polymorphism is associated with increased ulcerative colitis (UC) susceptibility in human patients [26]. *IL11* expression is increased in patients with mild UC, but decreased in patients with severe UC[27]. These findings suggest that IL-11 may promote colorectal cancer development, but could also attenuate colitis under certain conditions. Moreover, recent studies report that IL-11 plays a crucial role in fibrosis development in various organs, including the lung, heart, liver, and kidney[28, 29].

In the present study, we aimed to characterize IL-11-producing cells *in vivo*. We generated *Il11-Enhanced green fluorescence protein (Egfp)* reporter mice, and detected IL-11$^+$ cells in the colonic tumor tissues of a CAC mouse model and in $Apc^{Min/+}$ mice. Deletion of *Il11ra* or *Il11* attenuated CAC development in mice. When tumor organoids were transplanted into the colon, IL-11$^+$ cells appeared in the tumor tissues. Moreover, IL-11$^+$ cells rapidly appeared in the colon of mice after DSS treatment. IL-11$^+$ cells expressed stroma cell markers and genes associated with cell proliferation and tissue

repair, suggestive of colonic fibroblasts. IL-11 induced robust STAT3 phosphorylation in colonic fibroblasts, but not in colonic epithelial organoids. Using the human cancer database, we found that the genes enriched in IL-11$^+$ fibroblasts were elevated in human colorectal cancer, and that high expression of several of these genes was correlated with reduced disease-free survival among CRC patients. Together, our present results demonstrated that tumor cells induced IL-11$^+$ fibroblasts, and that a feed-forward loop between IL-11 and IL-11$^+$ fibroblasts may contribute to tumor development.

RESULTS

Characterization of IL-11^{+} Cells in CAC Using *Il11-Egfp* Reporter Mice

To characterize IL-11-producing (IL-11^{+}) cells *in vivo*, we generated transgenic mice in which *Egfp* expression was under control of the *Il11* gene promoter using a bacterial artificial chromosome (BAC) vector (Supplementary Fig. 1a). *Egfp* cDNA and a polyA signal were inserted in-frame in the second exon of the *Il11* gene (Supplementary Fig. 1a). As expected, *Il11* mRNA expression was correlated with *Egfp* mRNA expression in various tissues (Supplementary Fig. 1b, c). Notably, *Il11* mRNA expression was highest in the testis, and was very low in other tissues in mice under normal conditions (Supplementary Fig. 1b).

Although *Il11* mRNA expression is elevated in colorectal cancer among mice and human[16, 17], the origin of IL-11^{+} cells remains controversial. We used the *Il11-Egfp* reporter mice to monitor the appearance of IL-11^{+} cells in a CAC model. AOM administration followed by repeated exposure to DSS causes CAC development in mice[30, 31, 32, 33]. On day 77 after AOM/DSS administration, the *Il11-Egfp* reporter mice developed large tumors in the colon (Fig. 1a, b). At this time, we isolated tumor and

nontumor tissues, and examined the *Il11* mRNA expression by qPCR. *Il11* and *Egfp* mRNA expressions were elevated in tumor tissues compared to nontumor tissues from mice with AOM/DSS-induced CAC (Fig. 1c).

We next isolated and characterized IL-11$^+$ cells from tumors of *Il11-Egfp* reporter mice. We observed increased numbers of EGFP (IL-11)$^+$ cells in tumor tissues compared to nontumor tissues from the colon of AOM/DSS-treated *Il11-Egfp* reporter mice (Fig. 1d). While the majority of IL-11$^+$ cells expressed stroma cell markers, such as Thy1.2 and podoplanin, numerous IL-11$^+$ cells expressed CD45.2 or EpCAM (Fig. 1e). Immunohistochemistry (IHC) revealed IL-11$^+$ cells in stroma tissues surrounding tumor cells (Fig. 1f). IL-11$^+$ cells also expressed vimentin, collagen I, and collagen IV, but not αSMA (Supplementary Fig. 1d), suggesting that these cells were fibroblasts but not myofibroblasts. Notably, a few E-cadherin-positive tumor cells exhibited weak EGFP expression (Fig. 1g). Overall, these results suggest that the IL-11$^+$ cells constituted heterogenous cell populations, which might explain previous apparently inconsistent results showing that IL-11$^+$ cells were derived from hematopoietic, epithelial, or stromal cells[17, 24].

150 EGFP-positive cells were not detected in the colon of *Il11-Egfp* reporter mice
151 before AOM/DSS treatment (data not shown), possibly suggesting that small numbers
152 of resident IL-11^{+} cells might proliferate and expand *in situ*. Alternatively, IL-11^{-} cells
153 could be converted into IL-11^{+} cells after AOM/DSS treatment. To discriminate these
154 two possibilities, we investigated whether IL-11^{+} cells expressed the cell-proliferating
155 antigen Ki67. The majority of IL-11^{+} cells did not express Ki67 (Fig. 1h), supporting
156 the possibility that IL-11^{+} cells were derived from IL-11^{-} cells during tumor
157 development.

158

159 **Attenuated CAC Development in *Il11ra1*$^{-/-}$ and *Il11*$^{-/-}$ Mice**

160 A previous study reported attenuated CAC development in *Il11ra1*$^{-/-}$ mice[17].
161 Consistently, our present data confirmed the attenuation of AOM/DSS-induced CAC in
162 *Il11ra1*$^{-/-}$ mice compared to wild-type mice (Supplementary Fig. 2a). To further
163 substantiate that the IL-11/IL-11R-dependent signaling pathway contributed to CAC
164 development, we investigated *Il11*$^{-/-}$ mice. As we previously reported[34], *Il11*$^{-/-}$ mice
165 showed no abnormalities. When wild-type and *Il11*$^{-/-}$ mice were treated with

166 AOM/DSS, we observed attenuated CAC development in *Il11*$^{-/-}$ mice compared to
167 wild-type mice (Supplementary Fig. 2b). Moreover, reciprocal BM transfer
168 experiments revealed that *Il11* expression in non-hematopoietic cells might be
169 primarily responsible for the increased tumor numbers and tumor load in the colon
170 (Supplementary Fig. 2c, d), although *Il11* expression in hematopoietic cells also partly
171 contributed the increased tumor area in the colon (Supplementary Fig. 2c, d). We
172 focused our subsequent analyses on IL-11^{+} colonic fibroblasts, which are hereafter
173 referred to as IL-11^{+} colon cancer-associated fibroblasts (CAFs).
174
175 **IL-11^{+} CAFs Appear in Tumor Tissues in the Absence of Inflammation**
176 The above-described results suggested that tumor cells may have educated the
177 surrounding IL-11^{-} cells to become IL-11^{+} CAFs. An alternative possibility is that
178 IL-11^{-} cells might cell-autonomously become IL-11^{+} CAFs within the setting of an
179 inflammatory milieu triggered by DSS administration. To discriminate these
180 possibilities, we used two different inflammation-independent murine tumor models:
181 adenomatous polyps in *Apc*$^{Min/+}$ mice[33] and transplantation of tumor organoids into

182 wild-type mice. In *Apc*$^{Min/+}$ mice, *Il11* and *Egfp* mRNA expression levels were elevated
183 in colon tumors compared to nontumor tissues (Fig. 2a), and IL-11^{+} CAFs appeared in
184 stroma tissues surrounding tumor cells in the colon (Fig. 2b). Consistent with the results
185 of IHC, we found increased numbers of IL-11^{+} CAFs in the tumor tissues compared to
186 non-tumor tissues from the colon of *Apc*$^{Min/+}$ mice (Fig. 2c). Moreover, most IL-11^{+}
187 CAFs expressed podoplanin and Thy1.2, and small numbers of IL-11^{+} cells expressed
188 hematopoietic and epithelial cell markers (Fig. 2d). Again, we observed weak EGFP
189 expression in some E-cadherin-positive tumor cells themselves (Fig. 2e). Notably, most
190 IL-11^{+} CAFs were not Ki67^{+} (Fig. 2f). IL-11^{+} CAFs expressed vimentin, collagen I, and
191 collagen IV, but not αSMA (Fig. 2g).

192 We previously generated tumor organoids from the intestines of AKTP mice,
193 which exhibit mutations of *Apc, Kras, Tgfbr2,* and *Tp53* in intestinal epithelial cells [35].
194 These tumor organoids were transferred into the colon of *Il11-Egfp* reporter mice, and
195 we examined whether IL-11^{+} CAFs appeared along with tumor development
196 (Supplementary Fig. 3a). On day 30 post-transplantation, the tumor organoids had
197 developed into large tumors in the colon and, importantly, IL-11^{+} CAFs appeared in the

198 tumor tissues (Figure Supplementary Fig. 3b). Moreover, these IL-11$^+$ CAFs expressed
199 podoplanin and vimentin, but not CD45 or E-cadherin (Supplementary Fig. 3c).
200 Together, these results strongly support that tumor cells instructed IL-11$^-$ cells to
201 become IL-11$^+$ CAFs in the absence of inflammation.
202
203 **IL-11$^+$ Cells Appear in the Colon of DSS-Treated Mice and Express Stromal Cell**
204 **Marker**
205 To test whether inflammation alone induced IL-11$^+$ cell development, we treated
206 *Il11-Egfp* reporter mice with only DSS. *Il11* and *Egfp* expressions were very low in the
207 colon of untreated *Il11-Egfp* reporter mice, and were elevated in the colon of *Il11-Egfp*
208 reporter mice on day 7 after DSS treatment (Fig. 3a). IHC revealed that on day 6 after
209 DSS treatment, large numbers of IL-11$^+$ cells appeared in the subepithelial tissues,
210 where intestinal epithelial cells were detached due to severe inflammation (Fig. 3b).
211 Moreover, we detected the rapid appearance of IL-11$^+$ cells just one day after DSS
212 treatment (Fig. 3c). For a more detailed comparison of the phenotypes of IL-11$^+$ CAFs
213 in tumor tissues and the IL-11$^+$ cells that appeared in colitis, we used flow cytometry to

214 analyze the expressions of various cell surface markers. After DSS treatment, we
215 observed increased numbers of IL-11$^+$ cells in the colon (Fig. 3d). These IL-11$^+$ cells
216 expressed stroma cell markers, including Thy1.2, podoplanin, CD29, PDGFR-α,
217 ICAM-1, VCAM-1, and Sca-1, but not CD45.2, EpCAM, CD31, or Ter119 (Fig. 3e).
218 IL-11$^+$ cells were also positive for vimentin, collagen I, and collagen IV, but not αSMA
219 (Fig. 3f), suggesting that these cells were fibroblasts, but not myofibroblasts. Moreover,
220 these IL-11$^+$ cells did not incorporate 5-bromo-2′-deoxyuridine (BrdU), a hallmark of
221 cell proliferation, suggesting that they did not proliferate *in situ* (Fig. 3g). Together,
222 these findings suggest that inflammation alone was sufficient to induce IL-11$^+$ cell
223 development.
224
225 **IL-11$^+$ Cells Express Genes Associated with Cell Proliferation and Tissue Repair**
226 To further characterize the IL-11$^+$ cells that appeared in colitis, we used a cell sorter to
227 isolate IL-11$^+$ cells as EGFP$^+$ cells from the colon of DSS-treated *Il11-Egfp* reporter
228 mice. These sorted EGFP$^+$ cells were subjected to transcriptome analysis, and their gene
229 expression profiles were compared with those of EGFP$^-$ cells. Heat-map analysis

revealed different gene expression patterns in these two populations (Fig. 4a). A volcano plot showed significantly elevated expressions of several genes, including *Il11*, *Mmp3*, and *Timp1*, in IL-11^{+} cells compared to IL-11^{-} cells (Fig. 4b). Gene Ontology (GO) enrichment analysis revealed that EGFP^{+} cells exhibited enriched expressions of genes associated with cell proliferation, organ morphogenesis, angiogenesis, and wound healing (Fig. 4c). qPCR confirmed that IL-11^{+} cells showed elevated levels of cytokines (*Il6* and *Il11*), chemokines (*Ccl2* and *Ccl11*), and genes associated with organ development (*Hgf* and *Tnfsf11*) (Fig. 4d). We also detected elevated expression levels of genes associated with colorectal cancer susceptibility loci (e.g., *Grem, Bmp2*, and *Bmp4*) and tumor development and invasion (e.g., *Wnt5a, Ereg*, *Mmp3*, *Mmp13,* and *Timp1*) (Figure 4D).

Of note, two unique subsets of fibroblasts termed inflammation-associated fibroblasts (IAFs)[9] and cancer-associated fibroblasts (CAFs) with mediating chemotherapy resistance[10] have been recently reported in ulcerative colitis (UC) patients and chemotherapy-resistant cancer patients, respectively. To investigate the relationship between IL-11^{+} fibroblasts and IAFs or CAFs with mediating

246 chemotherapy resistance, we examined their hallmark gene expressions. We found
247 elevated expressions of *Il13ra2* and *Tnfsfr11b* (markers of IAFs), but not *Cd10* or
248 *Gpr77* (markers of CAFs with mediating chemotherapy resistance) in IL-11^{+} cells
249 compared to IL-11^{-} cells (Fig. 4e). These findings indicated that the IL-11^{+} cells
250 appearing in the colon of DSS-treated mice were phenotypically similar to the IAFs
251 observed in UC patients, but not CD10^{+}GPR77^{+} CAFs. Thus, these cells were referred
252 to as IL-11^{+} IAFs.

253 We next examined whether the gene expression profiles were similar between
254 IL-11^{+} IAFs and IL-11^{+} CAFs. The genes enriched in IL-11^{+} IAFs, including *Ccl2,*
255 *Osmr, Wnt5a, Ereg, Mmp13*, *Timp1*, and *Tnfrsf11b,* were also elevated in
256 AOM/DSS-induced tumor tissues (Supplementary Fig. 4). Although we did not examine
257 the gene expression profiles of IL-11^{+} CAFs from tumor tissues, our findings suggest
258 that IL-11^{+} IAFs may be phenotypically similar to IL-11^{+} CAFs.

259

260 **The MEK/ERK Pathway is Involved in *Il11* Upregulation in Tumor Tissues**

261 Since IL-11^{+} CAFs might promote tumor development, it is crucial to investigate the

mechanisms by which inflammation or tumor cells induce IL-11 expression. We previously reported that oxidative stress induces *Il11* mRNA expression in an ERK/Fra-1-dependent manner[22, 23]. Thus, we tested whether DSS treatment induced oxidative stress in the colon. We observed enhanced oxidative stress in colonic cells after DSS treatment, and found that an antioxidant, N-acetyl cysteine (NAC) administration attenuated this DSS-induced oxidative stress (Fig. 5a). Additionally, DSS-induced oxidative stress was ameliorated by administration of antibiotics (Abx) (Fig. 5b), suggesting that bacterial infection induces oxidative stress. Consistent with these findings, both an antioxidant, NAC and Abx blocked the DSS-induced upregulation of *Il11* mRNA (Fig. 5c, d). Furthermore, DSS induced ERK phosphorylation, which was blocked by administration of the MEK inhibitor trametinib or NAC, accompanied by downregulation of *Il11* expression (Fig. 5e–g). These results indicated that oxidative stress-dependent ERK activation might contribute to *Il11* expression in the colon. Although several studies report that TGFβ induces IL-11 production in various cells[20, 21], we found that neutralization of TGFβ signals using anti-TGFβ antibody did not block *Il11* expression in the colon after DSS treatment (Fig.

278 5h, i).

279 We next investigated whether *Il11* expression was induced in the tumor
280 microenvironment in a manner similar to those in DSS-induced colitis. Administration
281 of trametinib, but not Abx, NAC, or neutralizing antibody against TGFβ, decreased *Il11*
282 expression in CAC after AOM/DSS treatment (Fig. 5j–o). Moreover, we observed a
283 similar inhibitory effect of Trametinib, but not Abx, NAC, or neutralizing antibody
284 against TGFβ in colon tumors in $Apc^{min/+}$ mice (Supplementary Fig. 5a–f). Together,
285 these results suggested that *Il11* expression was induced in a MEK/ERK-dependent
286 manner, although the upstream signals that induce activation of the MEK/ERK pathway
287 could differ between cases of inflammation versus tumors. Of note, induction of *Il11* in
288 the colon might be independent of TGFβ in the tumor microenvironment at least under
289 our experimental conditions.

290

291 **IL-11 Preferentially Induces Signals to Fibroblasts**

292 Previous studies report that IL-11 induces signals in colonic epithelial cells and
293 fibroblasts[17, 29]. To determine which cells were the primary targets of IL-11, we

294 examined the *Il11ra1* expression on colonic fibroblasts and normal colonic epithelial
295 organoids. Since IL-22 induces signals in intestinal epithelial cells[36], we also examined
296 the IL-22 receptor expression on both cell types. Colonic epithelial organoids showed
297 high expression of *Il22r*, but not *Il11ra1*, while colonic fibroblasts exhibited high
298 expression of *Il11ra1*, but not *Il22ra1* (Fig. 6a). Consistently, robust STAT3
299 phosphorylation in colonic fibroblasts was induced by IL-11, but not IL-22 (Fig. 6b). To
300 further characterize IL-11-inducible genes *in vivo*, we injected IL-11R agonist into
301 wild-type mice[22], which induced upregulation of many genes in the colon (Fig. 6c–e),
302 some of which were enriched in IL-11$^+$ IAFs (Fig. 6e). We performed qPCR to verify
303 the induction of these genes (including *Hgf, Osmr, Rspo3*, *Mmp3, Timp1,* and *Pdpn*) in
304 the colon after injection of IL-11R agonist (Supplementary Fig. 6). It is likely that IL-11
305 released from colonic fibroblasts might activate IL-11$^+$ IAFs or CAFs in an autocrine or
306 paracrine manner. Overall, our findings suggested that expression of IL-11-stimulated
307 genes in IL-11$^+$ CAFs might further modulate the tumor microenvironment.
308
309 **Genes Enriched in IL-11$^+$ IAFs Show Elevated Expression in Human Colorectal**

Cancer

Assuming that the appearance of IL-11$^+$ CAFs was correlated with CAC development in mice (Fig. 1, 2), we hypothesized that the genes enriched in IL-11$^+$ IAFs might also be elevated in human colorectal cancer. We focused on genes with over two-fold greater expression in IL-11$^+$ IAFs compared to IL-11$^-$ cells (Fig. 4), and extracted 17 genes matching our criteria from the human cancer database (GSE33133). Intriguingly, subsets of genes elevated in IL-11$^+$ IAFs, including *HGF, TNFSF11, MMP3, MMP13,* and *TIMP1*, were significantly upregulated in colon cancer tissues compared to normal mucosa (Supplementary Fig. 7a).

Since many of the genes enriched in IL-11$^+$ IAFs were also upregulated in tumor tissues (Fig. 4d, e, Supplementary Fig. 7a), we hypothesized that the genes elevated in IL-11$^+$ IAFs, along with *IL11*, might critically affect the prognosis of cancer patients. Thus, we compared disease-free survival of colorectal cancer patients according to the expression levels of genes enriched in IL-11$^+$ IAFs. We found that reduced disease-free survival time was associated with higher expression of *IL6*, *MMP13*, and *TIMP1*, but not of *IL6/IL6R*, *IL11*, or *IL11/IL11R* (Supplementary Fig. 7b). Notably, higher

326 expression of *IL6/IL6R/IL11/IL11R/GP130* was associated with significantly diminished
327 disease-free survival time. These results suggested that prognosis of human colorectal
328 cancer patients may be critically determined by IL-11$^+$ IAFs and, possibly, by IL-11$^+$
329 CAFs, but not by IL-11.
330
331 **IL-11 Expression is Correlated with Progression of Human Cancers**
332 To characterize IL-11$^+$ cells in human colon tumor samples, we performed staining with
333 anti-human IL-11 antibody. First, we verified that anti-human IL-11 antibody detected
334 endogenous IL-11, using lysates of the human breast cancer cell line MDA-MB-231, in
335 the absence or presence of siRNA against human *Il11* (Fig. 7a). IL-11$^+$ cells were
336 scarcely detected in normal colonic tissues, but were numerous in adenomas and in
337 early and advanced colorectal cancer tissues (Fig. 7b). Intriguingly, the relative area of
338 IL-11$^+$ cells and the IL-11 signaling intensity were increased in advanced colon cancers
339 compared to normal tissues (Fig. 7c, d). Moreover, positive staining for IL-11 was
340 observed in vimentin-positive stromal cells, E-cadherin-positive tumor cells, and
341 CD45-positive hematopoietic cells (Fig. 7e). Thus, IL-11$^+$ cells comprised

342 heterogeneous cell populations in the tumor microenvironment, although the majority

343 were fibroblasts.

DISCUSSION

In the present study, we generated *Il11-Egfp* reporter mice to characterize IL-11$^+$ CAFs or IL-11$^+$ IAFs in different murine tumor and colitis models. We found that IL-11$^+$ cells in tumor tissues constituted heterogenous cell populations, including stromal, epithelial, and hematopoietic cells, and that *Il11ra*$^{-/-}$ or *Illl*$^{-/-}$ deletion attenuated CAC development in mice. Reciprocal BM transfer experiments revealed that stromal cells critically contributed to tumor progression; thus, we focused on IL-11$^+$ CAFs. IL-11 activated IL-11$^+$ colonic fibroblasts. Transcriptome analysis showed that IL-11$^+$ IAFs expressed genes associated with tissue repair and cell proliferation. Moreover, some of the genes enriched in IL-11$^+$ IAFs were elevated in human colorectal cancer tissues, and their high expression was associated with poor prognosis of human colorectal cancer. Thus, our results suggest that a feed-forward loop between IL-11 and IL-11$^+$ CAFs may contribute to tumor development.

The newly developed *Il11-Egfp* reporter mice enabled us to characterize the IL-11$^+$ IAFs and CAFs that appeared in mouse models of colitis and CAC, respectively. In the colitis model, IL-11$^+$ IAFs exclusively expressed stromal cell markers, such as

360 Thy1 and podoplanin. A recent cRNA-seq analysis of colon biopsies from healthy
361 individual and UC patients revealed that colon samples from UC patients exhibited a
362 unique subset of fibroblasts, termed IAFs, that express *IL11*, *IL24*, *IL13RA2,* and
363 *TNFSFR11B*[9]. Here we found elevated expression of these genes in IL-11$^+$ IAFs
364 compared to IL-11$^-$ cells. Thus, IL-11 is a hallmark of IAFs. Since IL-11$^+$ IAFs
365 expressed genes associated with cell proliferation and tissue repair, IL-11$^+$ IAFs might
366 contribute to colitis attenuation in human UC patients.

367 In contrast to in DSS-induced colitis, in tumor tissues, we detected numerous
368 IL-11$^+$ cells expressing epithelial or hematopoietic cell markers, including EpCAM or
369 CD45.2. Consistently, previous studies report that IL-11$^+$ cells are derived from stromal,
370 epithelial, or hematopoietic cells[17, 24]. Our present results revealed that IL-11$^+$, EpCAM$^+$,
371 and E-cadherin$^+$ epithelial cells might be tumor cells themselves, whereas we did not
372 fully investigate the nature and origin of CD45.2$^+$ cells. Future scRNA-seq analysis of
373 IL-11$^+$ cells will further elucidate the origin and characterization of heterogenous
374 populations of IL-11$^+$ cells in the tumor microenvironment.

375 Tumors cells may support tumor growth by educating the surrounding

376 fibroblasts, which are referred to as CAFs[8, 37, 38]. On the other hand, a recent study
377 reported that surface expression of CD10 and GPR77 may be markers of CAFs that
378 mediate chemotherapy resistance in human cancer through IL-6 and IL-8 production [10].
379 CD10 and GPR77 expression were not elevated in IL-11$^+$ IAFs or CAC in mice,
380 suggesting that IL-11$^+$ IAFs and possibly IL-11$^+$ CAFs might be different from human
381 CD10$^+$GPR77$^+$ CAFs.

382 Elucidation of the mechanisms underlying IL-11 production by stromal cells in
383 the tumor microenvironment may be crucial for understanding how tumor cells instruct
384 stromal cells. Previous studies demonstrate that TGFβ induces IL-11 upregulation in
385 various cell types[20, 21]. Indeed, we found that TGFβ stimulation induced IL-11
386 production by colonic fibroblasts. Moreover, in murine xenograft models, human tumor
387 cell lines that ectopically express human TGFβ1 can elicit IL-11$^+$ CAFs[24]. However, in
388 our present study, anti-TGFβ antibody treatment did not downregulate *Il11* expression
389 in colonic adenomas of *Apc*$^{min/+}$ mice, or in AOM/DSS-induced CAC. Furthermore,
390 culture supernatants of tumor organoids did not induce upregulated *Il11* expression by
391 colonic fibroblasts in the absence or presence of anti-TGFβ antibody. Overall, although

392 TGFβ *per se* was able to induce IL-11 production, TGFβ may not be involved in the
393 induction of IL-11^{+} CAFs in the tumor microenvironment, at least under our
394 experimental conditions. On the other hand, blockade of the ERK pathway attenuated
395 *Il11* expression in the colon of mice after DSS treatment, in colon adenomas of *Apc*$^{min/+}$
396 mice, and in AOM/DSS-induced CAC in mice. Thus, the signaling pathway(s) leading
397 to MEK/ERK activation might be critically involved in IL-11 production. Further
398 investigations are needed to address this subject.

399 Previous studies show that IL-11 and IL-22 induce proliferation and cell survival
400 of colonic epithelial cells through STAT3 activation[15, 36]. Indeed, under our
401 experimental conditions in colonic epithelial organoids, IL-22 induced strong STAT3
402 phosphorylation, whereas IL-11 induced only weak STAT3 phosphorylation. In sharp
403 contrast, IL-11 induced robust phosphorylation of STAT3 in colonic fibroblasts. Thus, it
404 appears that colonic fibroblasts produced IL-11 in response to factors from tumor cells,
405 which, in turn, activated and induced STAT3 phosphorylation in colonic fibroblasts in
406 an autocrine or paracrine manner. This feed-forward loop between IL-11 and IL-11^{+}
407 CAFs might contribute to tumor development.

408 CAC development was attenuated in *Il11ra1*$^{-/-}$ and *Il11*$^{-/-}$ mice treated with
409 AOM/DSS, but deletion of these genes did not dramatically affect tumor development
410 compared to in a previous study[17]. The reason for these discrepancies is currently
411 unknown. However, it is possible that the genetic background of the mice (C57/BL6 vs.
412 129/C57/BL6 mixed background) might affect the tumor cells' dependence on IL-11
413 signaling. On the other hand, our transcriptome analysis revealed that IL-11^{+} CAFs
414 expressed various genes associated with tissue repair and cell proliferation. Indeed, we
415 found that high expression of the genes enriched in IL-11^{+} IAFs (including *IL6*, *MMP3*,
416 and *TIMP1*, but not *IL11* itself) was associated with reduced disease-free survival of
417 CRC patients. Thus, it would be interesting to investigate whether depletion of IL-11^{+}
418 CAFs might have profound effects on colorectal cancer progression.
419

METHODS

Reagents

Recombinant mouse IL-11 (R&D), IL-22 (Biolegend), mouse TGFβ1 (Biolegend), N-acetyl cysteine (NAC) (Nakalai), and Trametinib (LC Laboratories) were purchased from the indicated sources. The following antibodies used in this study were obtained from the indicated sources: anti-phospho-ERK (4370, CST), anti-Ki67 (ab16667, Abcam), anti-GFP (GFP-Go-Af1480 or GFP-Rb-Af2020, Frontier Institute), anti-BrdU (BU1/75, BIO-RAD), anti-IL-11 (LS-C408373, LSBio), anti-CD45 (13917, CST), anti-CD45 (IR751, Dako), anti-podoplanin (127403, BioLegend), anti-α-SMA (ab5694, Abcam), anti-collagen I (ab34710, Abcam), anti-collagen IV (ab6586, Abcam), anti-E-cadherin (560062, BD Biosciences), anti-E-cadherin (NCH-38, Dako), anti-vimentin (9856, CST), anti-phospho-STAT3 (9145, CST), anti-STAT3 (SC-482, Santa Cruz), anti-β-Actin (622102, Biolegend), and anti-tubulin (T5168, Sigma-Aldrich). Anti-horseradish peroxidase (HRP) -conjugated anti-rabbit IgG (NA934), HRP-conjugated anti-rat IgG (NA935), and HRP-conjugated anti-mouse IgG (NA931) antibodies were from GE Healthcare. Alexa Fluor 488-conjugated donkey anti-rabbit IgG (A21206), Alexa Fluor 594-conjugated donkey anti-rabbit IgG

(A21207), Alexa Fluor Plus 594-conjugated donkey anti-rabbit IgG (A32754), Alexa Fluor 647-conjugated donkey anti-rabbit IgG (A31573), Alexa Fluor 594-conjugated donkey anti-mouse IgG (A21203), and Alexa Fluor 488-conjugated donkey anti-goat IgG (A11055) antibodies, and Alexa Fluor 594-conjugated streptavidin (S11227) were purchased from Invitrogen.

Unless otherwise indicated, the following antibodies used for flow cytometry were obtained from TONBO Biosciences; anti-CD11b (20-0112, clone M1/70), anti-CD16/CD32-mAb (2.4G2) (made in house), anti-CD24a (Biolegend, 101813, clone M1/69), anti-CD31 (eBioscience, 17-0311-82, clone 390), anti-CD34 (eBioscience, 13-0341-81, clone RAM34), anti-CD45.1 (35-0453, clone A20), anti-CD45.2 (20-0454, clone 104), anti-EpCAM (BioLegend, 118214, clone G8.8), anti-Thy1.2 (20-0903, clone 30-H12), anti-podoplanin (BioLegend, 127414, clone 8.1.1), anti-TER-119 (BioLegend, 116212, clone TER-119), anti-MHC Class II (Miltenyi Biotec, 130-102-139, clone M5/114.15.2), anti-ICAM-1 (BD Biosciences, 561605, clone 3E2), anti-VCAM-1 (BioLegend, 105718, clone 429), anti-Sca-1 (BioLegend, 122512, clone

452 E13161.7), anti-Lyve1 (eBioscience, 50-0443-80, clone ALY7), anti-PDGFRα
453 (eBioscience, 17-1401-81, clone APA5), and Streptavidin APC (eBioscience).

454 The hybridoma cell line (1D11)[39] that produces neutralizing antibody against
455 all TGFβ isoforms (β1, β2, and β3) was purchased from ATCC, and anti-TGFβ
456 antibody was produced in house. Control mouse IgG was purchased from
457 Sigma-Aldrich (I5381).

458

459 **Mice**

460 *Il11*$^{-/-}$ mice (generated in our lab) and *Il11ra1*$^{-/-}$ mice (provided by L. Robb) were
461 previously described[34 40]. *Apc*$^{min/+}$ (002020) were purchased from Jackson Lab.
462 C57BL/6 (CD45.2^{+}) and C57BL/6-SJL (CD45.1^{+}) mice were purchased from
463 Japan-SLC.

464 Mice in different cages or derived from different sources were cohoused for 2
465 weeks for normalization of the microbiota composition before experiments. All animals
466 were housed and maintained under specific pathogen-free conditions in the animal
467 facility at Juntendo University School of Medicine or Toho University School of

Medicine. All experiments were performed according to the guidelines approved by the Institutional Animal Experiment Committee of Juntendo University School of Medicine or Toho University School of Medicine (19-51-414, 19-51-411).

Generation of *Il11-Egfp* reporter mice

The *Egfp* reporter gene was introduced into the BAC clone (RP23-285B12) by two-step Red/ET recombineering technology according to the manufacturer's protocol (Gene Bridges). In the first step, a *rpsL-neo* cassette included in the kit was amplified by PCR using a primer set (*Il11*-ET1-F2: ACTCCCTCAGACCCAGAGTTTGGCCTGATTTCTCCCTTCTGTCCACAGGTGG CCTGGTGATGATGGCGGGATCG and *Il11*-ET1-R2: ACGACTCTATCTGGCCAGAGGCTCAGCACCACCAGGACCAGGCGACAAACT CAGAAGAACTCGTCAAGAAGGCG) and inserted into the target region of the BAC clone. In a second step, the *rpsL-neo* cassette in the modified BAC clone was replaced with *Egfp-polyA* cassette which was amplified from *Egfp*-expression vector (pAWZ) using a primer set (*Il11*-ET2-F2:

484 ACTCCCTCAGACCCAGAGTTTGGCCTGATTTCTCCCTTCTGTCCACAGGTATG

485 GTGAGCAAGGGCGAG and *Il11*-ET2-R2:

486 ACGACTCTATCTGGCCAGAGGCTCAGCACCACCAGGACCAGGCGACAAACct

487 CTAGTGGATCATTAACGCTTAC). A resultant clone designated as *IL11-Egfp* was

488 verified by restriction digestion of BAC DNA and by sequencing.

489 Intracytoplasmic sperm injection (ICSI) was performed as previously

490 described with slightly modifications[41]. The mixture of sperm and *Il11-Egfp* DNA was

491 diluted with Hepes-modified CZB containing 12% polyvinylpyrrolidone

492 (Sigma-Aldrich) before being used for ICSI. Injections were performed by

493 micromanipulators (Leica) with a PMM-150 FU piezo-impact drive unit (Prime Tech)

494 using a blunt-ended mercury-containing injection pipette. After discarding the midpiece

495 and tail, the head of spermatozoa was injected into an oocyte from C57/BL6 mice.

496 Oocytes matured into two-cell stage embryos at 24 hours after injection, and then

497 two-cell stage embryos were transferred to oviducts of pseudopregnant females.

498 Transgenic founders were backcrossed to C57/BL6J mice for several generations.

499 Among them, one line exhibited an intimate correlation of *Il11* and *Egfp* expressions

were selected and used for further experiments.

Induction of DSS-induced colitis and colitis-associated cancer (CAC) in mice

Nine- to fifteen-week-old wild-type or *Il11-Egfp* reporter mice received 1.5 % DSS (MW: 36,000-50,000 D; MP Biomedicals) *ad libitum* in drinking water for 5 days, which then was changed to regular water. To reduce gut commensal microflora, mice received mixtures of antibiotics in drinking water containing ampicillin (1 g/L, Sigma-Aldrich), kanamycin (0.4 g/L, Sigma-Aldrich), gentamicin (0.035 g/L, Sigma-Aldrich), metronidazole (0.215 g/L, Sigma-Aldrich), vancomycin (0.18 g/L, Sigma-Aldrich), and colistin (0.042 g/L, Sigma-Aldrich). Administration of antibiotics into mice started at 4 weeks before DSS treatment and continued during DSS treatment. To attenuate oxidative stress in DSS-treated mice, mice received NAC (10 g/L) along with DSS in drinking water for 5 days. To neutralize TGFβ in DSS-treated mice, mice were intraperitoneally injected with anti-TGFβ antibody (1D11) or control mouse IgGs (5 mg/kg) on day 2 and day 4 after DSS treatment. To inhibit ERK activation in DSS-treated mice, a MEK inhibitor, Trametinib (2 mg/kg) was administered into mice

by gavage at 30 and 6 hours before the start of DSS treatment at a fine suspension in 0.5% Hydroxypropyl Cellulose (Alfa Aesar) and 0.2 % Tween-80.

To induced CAC, 9- to 15-week-old mice were intraperitoneally injected with 10 mg/kg AOM (Sigma-Aldrich). One week later, mice received 1.5 % DSS *ad libitum* in drinking water for 5 days, followed by 2 weeks of regular water, and this was repeated for two additional cycles. To reduce numbers of commensal bacteria and oxidative stress in AOM/DSS-treated mice or $Apc^{min/+}$ mice, we administered mixtures of antibiotics and NAC into the indicated mice for the last 8 weeks and 4 weeks just before sacrifice, respectively. Trametinib (2mg/kg) (−6 and −30 hours) or anti-TGFβ antibody (5 mg/kg) (on day −1, −3, −5) were administered into AOM/DSS-treated mice or $Apc^{min/+}$ mice at the indicated days just before sacrifice.

Flow cytometry

To isolate IL-11^{+} cells, the colon was removed from DSS-treated *Il11-Egfp* reporter mice. Then, the colon was minced with scissors and digested in RPMI 1640 containing 100 U/mL Penicillin and 100 μg/mL Streptomycin, 1mg/mL Collagenase (Wako), 50

μg/mL DNase (Roche), 0.5 mg/mL Dispase (Roche), and 2% (v/v) fetal bovine serum (FBS, Gibco) for 60 min. Single cell suspensions were prepared, and cells were stained with the indicated antibodies and analyzed by LSRFortessa X-20 (BD Biosciences) or BD Verse (BD Biosciences). Data were processed by FlowJo software (FlowJo). To further characterize IL-11^{+} cells, EGFP^{+} cells were sorted by MoFlo Astrios cell sorter (Beckman Coulter) and subjected to microarray analysis.

To isolate IL-11^{+} cells from tumors in the colon of *Il11-Egfp* reporter mice treated with AOM/DSS or *Apc*$^{min/+}$*;Il11-Egfp* mice, tumor tissues were removed from non-tumor tissues. Then, single cell suspension from tumor tissues was prepared as described above. Cells were stained with the indicated antibodies and expression of various cell surface markers on GFP^{+} cells were analyzed by flow cytometry.

Generation of bone marrow chimeras

After BM cells were prepared from *Il11*$^{+/+}$ or *Il11*$^{-/-}$ mice (CD45.2), 3-5 x 10^{6} BM cells were transferred to 8-week-old recipient mice [C57BL/6-SJL mice (CD45.1)] that had been exposed to lethal irradiation (9.0 Gray). In reciprocal BM transfer experiments,

548 BM cells from wild-type C57BL/6-SJL mice (CD45.1) were transferred to *Il11*$^{+/+}$ or
549 *Il11*$^{-/-}$ mice (CD45.2) that had been exposed to lethal irradiation (9.0 Gray). At 2 to 3
550 months after transfer, peripheral blood mononuclear cells were collected and stained
551 with FITC-conjugated anti-CD45.1 and allophycocyanin (APC)-conjugated
552 anti-CD45.2 antibodies. The chimerism of bone marrow cells was calculated by
553 counting numbers of CD45.1^{+} and CD45.2^{+} by flow cytometry. Average chimerisms
554 were more than 90 %.
555
556 **Quantitative PCR (qPCR) Assays**
557 Total RNAs were extracted from the indicated tissues of mice by using TRI Reagent
558 (Molecular Research Center) or Sepasol II Super (Nacalai Tesque), and cDNAs were
559 synthesized with the RevertraAce qPCR RT Kit (Toyobo). To remove residual DSS,
560 mRNAs prepared from the colon of mice treated with DSS were further purified by
561 LiCl precipitation as described previously [42]. Quantitative polymerase chain reaction
562 (qPCR) analysis was performed with the 7500 Real-Time PCR detection system with
563 CYBR green method of the target genes together with murine *Hprt* an internal control

564 with 7500 SDS software (Thermo Fisher Scientific). The primers used in this study are
565 shown in Table S1.
566
567 **Microarray analysis**
568 We compared gene expression profiles of RNAs from EGFP-positive and negative cells
569 from the colon of *Il11-Egfp* reporter mice. $EGFP^+$ and $EGFP^-$ cells were sorted from the
570 colon of *Il11-Egfp* mice (n = 3 mice) on day 7 after DSS administration, total RNAs
571 were extracted using TRI-reagent according to the manufacturer's instructions
572 (Molecular Research Center). Purified RNAs were subjected to a LiCl purification to
573 remove residual DSS. cDNA was synthesized with the Ambion WT Expression Kit
574 (Affymetrix) and labeled with GeneChip WT Terminal Labeling Kit (Affymetrix)
575 according to the manufacturer's protocol. Affymetrix GeneChip Hybridization wash
576 stain kit was used to hybridize samples to GeneChip Mouse Gene ST 1.0 ST Array
577 (Affymetrix). Signals were scanned with the Genechip Scanner 3000 7G, and obtained
578 data were analyzed with Affymetrix Expression Console software (Affymetrix). The
579 gene expression was analyzed using GeneSpring (Silicon Genetics). Functional

580 enrichment analysis of differentially expressed genes from the data of microarray
581 analysis was performed using DAVID Bioinformatics Resources[43, 44]. Data were
582 deposited in NCBI as a GSE140411.

583 To identify target genes by IL-11 in the colon, we intravenously injected 10
584 μg of IL-11R agonist into wild-type mice (n=2-3 mice). Generation, purification, and
585 characterization of IL-11R agonist were described previously[22]. Mice were sacrificed at
586 3 hours after injection. Total RNAs were extracted from the colon of mice by using
587 Sepasol II Super. Labeled cRNA were prepared from total RNA using the Agilent's
588 Quick Amp Labeling Kit (Agilent). Following fragmentation, cRNA were hybridized to
589 SurePrint G3 Mouse Gene Expression 8x60K (Agilent) according to the manufacturer's
590 instruction. Raw data were extracted using the software provided by Agilent Feature
591 Extraction Software (v11.0.1.1). The raw data for same gene was then summarized
592 automatically in Agilent feature extraction protocol to generate raw data text file,
593 providing expression data for each gene probed on the array. Array probes that have
594 Flag A in samples were filtered out. Selected processed signal value was transformed by
595 logarithm and normalized by quantile method. Statistical significance of the expression

596 data was determined using fold change and LPE test in which the null hypothesis was
597 that no difference exists among 2 groups. Hierarchical cluster analysis was performed
598 using complete linkage and Euclidean distance as a measure of similarity.
599 Gene-Enrichment and Functional Annotation analysis for significant probe list was
600 performed using Gene Ontology (http://geneontology.org). All data analysis and
601 visualization of differentially expressed genes was conducted using R 3.0.2
602 (www.r-project.org). Data were deposited in NCBI as a GEO accession number
603 GSE141643.
604
605 **Immunohistochemistry (IHC)**
606 Tissues were fixed in 10% formalin and embedded in paraffin blocks.
607 Paraffin-embedded colonic sections were used for H&E staining, immunohistochemical,
608 and immunofluorescence analyses. For immunohistochemistry, paraffin-embedded
609 sections were treated with Instant Citrate Buffer Solution (RM-102C, LSI Medicine) or
610 Target Retrieval Solution (S1699, Dako) as appropriate to retrieve antigen. Then tissue
611 sections were stained with the indicated antibodies, followed by visualization of

612 Alexa-conjugated secondary antibodies, or biotin-conjugated secondary antibodies
613 followed by Streptavidin-HRP (Vector Laboratories).

614 In human tumor samples, tissue sections were preincubated with MaxBlock™
615 Autofluorescence Reducing Kit (MaxVision Biosciences) according to the
616 manufacturer's instructions. After blocking, tissue sections were stained with the
617 indicated antibodies as described above.

618 Pictures were obtained with an all-in-one microscope (BZ-X700, Keyence) or
619 BX-63 (Olympus) and analyzed with BZ-X Analyzer (Keyence) or cellSens (Olympus)
620 software. Confocal microscopy was performed on an LSM 880 (Zeiss) or A1R (Nikon).
621 Images were processed and analyzed using the ZEN software (Zeiss) or the
622 NIS-Elements (Nikon).

623

624 **Histological scoring of severity of colitis**

625 Severity of colitis was evaluated by the following criteria, including infiltration of
626 inflammatory cells and the degree of tissue damage as previously described [45].
627 Infiltration of inflammatory cells; 0, the presence of rare inflammatory cells in the

colonic lamina propria; 1, increased numbers of inflammatory cells; 2, confluence of inflammatory cells; 3, extending of inflammatory cells into the submucosa and transmural extension of the inflammatory cell infiltrate. The degree of tissue damage; 0, absence of mucosal damage; 1, discrete focal lymphoepithelial lesions; 2, mucosal erosion and ulceration; 3, extensive mucosal damage and extension through deeper structure of the intestinal tract wall. Total severity scores ranging from 0 to 6 represent that 0 and 6 indicate no changes and extensive cell infiltration with tissue damage, respectively.

Organoid Culture and transplantation of tumor organoids

Mouse colon organoids were established from isolated crypts of wild-type mice as previously described with slight modification[46]. Obtained colonic organoids were cultured in Advanced DMEM/F12 (Thermo Fisher Scientific) containing 10 mM HEPES (Thermo Fisher Scientific), 1 x GlutaMAX (Thermo Fisher Scientific), 1 x B27 (Thermo Fisher Scientific), N-acetyl cysteine (1 μM), murine epidermal growth factor (50 ng/mL, Peprotech), murine Noggin (100 ng/mL, Peprotech), 0.5 mM A83-01

644 (Tocris), 3 μM SB202190 (Sigma), 1 μM nicotinamide (Sigma), Afamin and
645 Wnt3A-condition medium (CM) (final concentration of 50%) which was provided by J.
646 Takagi[47] and R-spondin 1-CM (final concentration of 10%) (Trevigen).

647 The small intestinal tumor organoids from
648 *villin-CreER-Apc*$^{min/+}$*-Kras*$^{+/LSL-G12D}$*-Tgfbr2*$^{flox/flox}$*-Tp53*$^{+/LSL-R270H}$ (AKTP) mice were
649 described previously [35]. AKTP organoids were cultured in Advanced DMEM/F12
650 containing 10 mM HEPES, 1 x GlutaMAX, 1 x B27, N-acetyl cysteine (1 μM), murine
651 epidermal growth factor (50 ng/mL), murine Noggin (100 ng/mL).

652 For transplantation, AKTP organoids were mechanically dissociated, and 3 x
653 10^5 organoid cells mixed in Matrigel were injected into the subepithelial tissues of the
654 rectum of *Il11-Egfp* reporter mice. At five weeks after transplantation, tumors were
655 removed and subjected to histological analysis.

656

657 **Isolation and stimulation of colonic fibroblasts**

658 To isolate colonic fibroblasts, single cell suspensions were prepared as described above
659 and cultured in DMEM containing 10% FBS, 1% GlutaMAX (Thermo Fisher

660 Scientific), 10 mM HEPES, 1% MEM Non-Essential Amino Acids Solution (100x)
661 (Nacalai Tesque), 100 U/mL Penicillin, 100 μg/mL Streptomycin, and 2.5 μg/mL of
662 Amphotericin B (Sigma). Culture medium was changed every day until colonic
663 fibroblasts started to grow spontaneously.

664 To detect phosphorylation of STAT3 in colonic fibroblasts, colonic fibroblasts
665 were stimulated with the indicated concentrations of IL-11 or IL-22 for 30 min. Total
666 and phosphorylated STAT3 were analyzed by Western blotting.

667

668 **Western Blotting**

669 Cells were lysed in a RIPA buffer (50mM Tris-HCl, pH 8.0, 150mM NaCl, 1% Nonidet
670 P-40, 0.5% deoxycholate, 0.1% SDS, 25 mM β-glycerophosphate, 1mM sodium
671 orthovanadate, 1mM sodium fluoride, 1 mM PMSF, 1 μg/ml aprotinin, and 1 μg/ml
672 leupeptin). After centrifugation, cell lysates were subjected to SDS-PAGE and
673 transferred onto polyvinylidene difluoride membranes (Millipore). The membranes
674 were immunoblotted with the indicated antibodies. The membranes were developed
675 with Super Signal West Dura extended duration substrate (Thermo Scientific) and
676 analyzed by Amersham Biosciences imager 600 (GE Healthcare). In some experiments,

677 blots were quantified using freeware program Fiji.

678

679 **Enzyme-linked immunosorbent assay (ELISA)**

680 Concentrations of murine IL-11 in the culture supernatants were determined by ELISA

681 according to the manufacturers' instruction (R&D Systems).

682

683 **Knockdown of *Il11* by siRNAs**

684 A human breast cancer cell line, MDA-MB-231 cells were provided by T. Sakamoto.

685 MDA-MB-231 cells were maintained in DMEM containing 10% FBS. MDA-MB-231

686 cells were transfected with control or *Il11* siRNAs using Lipofectamine 2000

687 (Invitrogen) at a final concentration of 50 nM. At 36 h after transfection, knockdown

688 efficiency of IL-11 by siRNAs was analyzed by immunoblotting with anti-IL-11

689 antibody using cell lysates. Stealth RNAi^{TM} siRNAs Negative Control, Med GC and

690 human *Il11,* NM_000641.3 (HSS179893, HSS179894, HSS179895) were purchased

691 from Thermo Fisher Scientific.

692

693 **Comparison of the expression of enriched genes in IL-11$^+$ IAFs between human**

694 **normal mucosa and colon cancer tissues**

695 The publicly available data set (GSE33113) was obtained from the Gene Expression

696 Omnibus (GEO). This data set contains gene expression data from 90 colon cancer

697 patients and 6 healthy persons. The expression data of enriched genes in IL-11$^+$ IAFs

698 was retrieved from the data set (GSE33113) and their signaling intensities of each gene

699 in normal mucosa and colon cancer tissues were compared.

700

701 **Survival analysis**

702 Two publicly available data sets (GSE17536 and GSE17537) were obtained from the

703 Gene Expression Omnibus (GEO). These data sets contain gene expression data and

704 disease-free survival information from 232 primary CRC patients. The expression levels

705 of enriched genes in IL-11$^+$ IAFs in these data sets was classified by the hierarchical

706 clustering. Each enriched gene in IL-11$^+$ IAFs was correlated with survival using the

707 Kaplan-Meier method. Statistical significance was analyzed by Mantel-Cox log-rank

708 test. R software was used for all statistical analysis.

709

710 **Human colorectal cancer tissues**

711 Human colon tumors and adjacent normal tissues were obtained from Toho University
712 Omori Medical Center and analyzed in accordance with approval by the Ethics
713 Committee of Toho University School of Medicine (A16111). Colon tumors included 10
714 cases of adenomas, 10 cases of early cancers, and 10 cases of advanced cancers.
715 Histological assessment of adenomas and adenocarcinomas was according to the
716 guidelines of the World Health Organization [48]. Early and advanced colon cancers were
717 determined according to the TNM criteria (pT1, early cancer; pT2-4, advanced
718 cancers)[49] .

719

720 **Statistical analysis**

721 Statistical significance was determined by the unpaired two-tailed Student's *t*-test,
722 Mann-Whitney U test, two-way ANOVA with Boniferroni's test, or one-way ANOVA
723 with Tukey's post-hoc test, Mantel-Cox log-rank test as indicated. *$p < 0.05$ was
724 considered to be statistically significant. All statistical analysis was performed with

725 Graph Pad Prism 7 software (GraphPad Software).

726

727

728

729

730

731

ACKNOWLEDGEMENTS

We thank T. Sakamoto for MDA-MB-231 cells. We also thank Y. Kurashima, H. Kiyono, M. Kikkawa, M. Aoki, A. Nakajima, E. Tosti, and L.S. Lopez for technical advice. This work was supported in part by Grants-in-Aid for Scientific Research (B) 17H04069 (to HN); Young Scientists (B) 17K15626 (to TN); Grants-in-Aid for Scientific Research (C) 26460397 (to TN); Challenging Exploratory Research 17K19533 (to HN) from Japan Society for the Promotion of Science (JSPS); Scientific Research on Innovative Areas 26110003 (to HN); the Japan Agency for Medical Research and Development (AMED) through AMED-CREST (JP19gm1210002, to HN); Private University Research Branding project (to TM and HN) from the MEXT (Ministry of Education, Culture, Sports, Science and Technology), Japan; and research grants from the Uehara Memorial Foundation (to TN) and the Takeda Science Foundation (to TN).

AUTHOR CONTRIBUTIONS

T.N. and H.N. designed research; T.N., Y.D., W.T., M.O., D.O., S.Y., M.K., E.N., Y.K., S.A-A., M.H., N.I., and N.T. performed research; M.N., M.O., H.Y., K.S., and T.M.

748 contributed to new reagents/analytical tools; T.N., Y.D., W.T., D.O., N.I., and H.N.

749 analyzed data; T.N., N.I., and H.N. wrote the paper.

750

751 **CONFLICT OF INTEREST**

752 The authors declare that they do not have competing financial interests.

753

754

755

756

REFERENCES

1. Peterson LW, Artis D. Intestinal epithelial cells: regulators of barrier function and immune homeostasis. *Nat Rev Immunol* **14**, 141-153 (2014).

2. Leoni G, Neumann PA, Sumagin R, Denning TL, Nusrat A. Wound repair: role of immune-epithelial interactions. *Mucosal Immunol* **8**, 959-968 (2015).

3. Kurashima Y, Kiyono H. Mucosal Ecological Network of Epithelium and Immune Cells for Gut Homeostasis and Tissue Healing. *Annu Rev Immunol* **35**, 119-147 (2017).

4. Powell DW, Pinchuk IV, Saada JI, Chen X, Mifflin RC. Mesenchymal cells of the intestinal lamina propria. *Annu Rev Physiol* **73**, 213-237 (2011).

5. Nowarski R, Jackson R, Flavell RA. The Stromal Intervention: Regulation of Immunity and Inflammation at the Epithelial-Mesenchymal Barrier. *Cell* **168**, 362-375 (2017).

6. Isella C*, et al.* Stromal contribution to the colorectal cancer transcriptome. *Nat Genet* **47**, 312-319 (2015).

7. Calon A*, et al.* Stromal gene expression defines poor-prognosis subtypes in colorectal cancer. *Nat Genet* **47**, 320-329 (2015).

8. Koliaraki V, Pallangyo CK, Greten FR, Kollias G. Mesenchymal Cells in Colon Cancer. *Gastroenterology* **152**, 964-979 (2017).

9. Smillie CS*, et al.* Intra- and Inter-cellular Rewiring of the Human Colon during Ulcerative Colitis. *Cell* **178**, 714-730.e722 (2019).

10. Su S*, et al.* CD10(+)GPR77(+) Cancer-Associated Fibroblasts Promote Cancer

Formation and Chemoresistance by Sustaining Cancer Stemness. *Cell* **172**, 841-856 e816 (2018).

11. Putoczki T, Ernst M. More than a sidekick: the IL-6 family cytokine IL-11 links inflammation to cancer. *J Leukoc Biol* **88**, 1109-1117 (2010).

12. Jones SA, Jenkins BJ. Recent insights into targeting the IL-6 cytokine family in inflammatory diseases and cancer. *Nat Rev Immunol* **18**, 773-789 (2018).

13. West NR. Coordination of Immune-Stroma Crosstalk by IL-6 Family Cytokines. *Front Immunol* **10**, 1093 (2019).

14. Gibson DL*, et al.* Interleukin-11 reduces TLR4-induced colitis in TLR2-deficient mice and restores intestinal STAT3 signaling. *Gastroenterology* **139**, 1277-1288 (2010).

15. Kiessling S*, et al.* Functional expression of the interleukin-11 receptor alpha-chain and evidence of antiapoptotic effects in human colonic epithelial cells. *J Biol Chem* **279**, 10304-10315 (2004).

16. Yoshizaki A, Nakayama T, Yamazumi K, Yakata Y, Taba M, Sekine I. Expression of interleukin (IL)-11 and IL-11 receptor in human colorectal adenocarcinoma: IL-11 up-regulation of the invasive and proliferative activity of human colorectal carcinoma cells. *Int J Oncol* **29**, 869-876 (2006).

17. Putoczki TL*, et al.* Interleukin-11 is the dominant IL-6 family cytokine during gastrointestinal tumorigenesis and can be targeted therapeutically. *Cancer Cell* **24**, 257-271 (2013).

18. Molet S*, et al.* IL-17 is increased in asthmatic airways and induces human bronchial fibroblasts to produce cytokines. *J Allergy Clin Immunol* **108**, 430-438 (2001).

19. Andoh A, *et al.* Interleukin-22, a member of the IL-10 subfamily, induces inflammatory responses in colonic subepithelial myofibroblasts. *Gastroenterology* **129**, 969-984 (2005).

20. Bamba S, Andoh A, Yasui H, Makino J, Kim S, Fujiyama Y. Regulation of IL-11 expression in intestinal myofibroblasts: role of c-Jun AP-1- and MAPK-dependent pathways. *Am J Physiol Gastrointest Liver Physiol* **285**, G529-538 (2003).

21. Tang W, Yang L, Yang YC, Leng SX, Elias JA. Transforming growth factor-beta stimulates interleukin-11 transcription via complex activating protein-1-dependent pathways. *J Biol Chem* **273**, 5506-5513 (1998).

22. Nishina T, *et al.* Interleukin-11 links oxidative stress and compensatory proliferation. *Sci Signal* **5**, ra5 (2012).

23. Nishina T, *et al.* Critical Contribution of Nuclear Factor Erythroid 2-related Factor 2 (NRF2) to Electrophile-induced Interleukin-11 Production. *J Biol Chem* **292**, 205-216 (2017).

24. Calon A, *et al.* Dependency of colorectal cancer on a TGF-beta-driven program in stromal cells for metastasis initiation. *Cancer Cell* **22**, 571-584 (2012).

25. Zhang X, *et al.* IL-11 Induces Th17 Cell Responses in Patients with Early Relapsing-Remitting Multiple Sclerosis. *J Immunol* **194**, 5139-5149 (2015).

26. Klein W, *et al.* A polymorphism in the IL11 gene is associated with ulcerative colitis. *Genes Immun* **3**, 494-496 (2002).

27. Sabzevary-Ghahfarokhi M, *et al.* The expression analysis of Fra-1 gene and IL-11 protein in Iranian patients with ulcerative colitis. *BMC Immunol* **19**, 17 (2018).

28. Strikoudis A, *et al.* Modeling of Fibrotic Lung Disease Using 3D Organoids Derived from Human Pluripotent Stem Cells. *Cell Rep* **27**, 3709-3723 e3705 (2019).

29. Schafer S, *et al.* IL-11 is a crucial determinant of cardiovascular fibrosis. *Nature* **552**, 110-115 (2017).

30. Neufert C, Becker C, Neurath MF. An inducible mouse model of colon carcinogenesis for the analysis of sporadic and inflammation-driven tumor progression. *Nat Protoc* **2**, 1998-2004 (2007).

31. Tanaka T, Kohno H, Suzuki R, Yamada Y, Sugie S, Mori H. A novel inflammation-related mouse colon carcinogenesis model induced by azoxymethane and dextran sodium sulfate. *Cancer Sci* **94**, 965-973 (2003).

32. Moser AR, Pitot HC, Dove WF. A Dominant Mutation That Predisposes to Multiple Intestinal Neoplasia in the Mouse. *Science* **247**, 322-324 (1990).

33. Su LK, *et al.* Multiple Intestinal Neoplasia Caused by a Mutation in the Murine Homolog of the Apc Gene. *Science* **256**, 668-670 (1992).

34. Deguchi Y, *et al.* Generation of and characterization of anti-IL-11 antibodies using newly established Il11-deficient mice. *Biochem Biophys Res Commun* **505**, 453-459 (2018).

35. Sakai E, *et al.* Combined Mutation of Apc, Kras, and Tgfbr2 Effectively Drives Metastasis of Intestinal Cancer. *Cancer Res* **78**, 1334-1346 (2018).

36. Pickert G, *et al.* STAT3 links IL-22 signaling in intestinal epithelial cells to mucosal wound healing. *J Exp Med* **206**, 1465-1472 (2009).

37. Yoshida GJ, Azuma A, Miura Y, Orimo A. Activated Fibroblast Program Orchestrates Tumor Initiation and Progression; Molecular Mechanisms and the

887 Associated Therapeutic Strategies. *Int J Mol Sci* **20**, (2019).
888
889 38. Turley SJ, Cremasco V, Astarita JL. Immunological hallmarks of stromal cells in
890 the tumour microenvironment. *Nat Rev Immunol* **15**, 669-682 (2015).
891
892 39. Dasch JR, Pace DR, Waegell W, Inenaga D, Ellingsworth L. Monoclonal
893 antibodies recognizing transforming growth factor-beta. Bioactivity
894 neutralization and transforming growth factor beta 2 affinity purification. *J*
895 *Immunol* **142**, 1536-1541 (1989).
896
897 40. Nandurkar HH, Robb L, Tarlinton D, Barnett L, Kontgen F, Begley CG. Adult
898 mice with targeted mutation of the interleukin-11 receptor (IL11Ra) display
899 normal hematopoiesis. *Blood* **90**, 2148-2159 (1997).
900
901 41. Kimura Y, Yanagimachi R. Intracytoplasmic sperm injection in the mouse. *Biol*
902 *Reprod* **52**, 709-720 (1995).
903
904 42. Viennois E, Chen F, Laroui H, Baker MT, Merlin D. Dextran sodium sulfate
905 inhibits the activities of both polymerase and reverse transcriptase: lithium
906 chloride purification, a rapid and efficient technique to purify RNA. *BMC Res*
907 *Notes* **6**, 360 (2013).
908
909 43. Huang DW, Sherman BT, Lempicki RA. Bioinformatics enrichment tools: paths
910 toward the comprehensive functional analysis of large gene lists. *Nucleic Acids*
911 *Research* **37**, 1-13 (2009).
912
913 44. Huang DW, Sherman BT, Lempicki RA. Systematic and integrative analysis of
914 large gene lists using DAVID bioinformatics resources. *Nature Protocols* **4**,
915 44-57 (2009).
916
917 45. Lochner M*, et al.* Microbiota-induced tertiary lymphoid tissues aggravate
918 inflammatory disease in the absence of RORgamma t and LTi cells. *J Exp Med*
919 **208**, 125-134 (2011).

46. Sato T*, et al.* Long-term expansion of epithelial organoids from human colon, adenoma, adenocarcinoma, and Barrett's epithelium. *Gastroenterology* **141**, 1762-1772 (2011).

47. Mihara E*, et al.* Active and water-soluble form of lipidated Wnt protein is maintained by a serum glycoprotein afamin/alpha-albumin. *Elife* **5**, (2016).

48. Aaltonen LA, Hamilton SR, World Health Organization., International Agency for Research on Cancer. *Pathology and genetics of tumours of the digestive system*. IARC Press ; Oxford University Press (distributor (2000).

49. Sobin LH, Gospodarowicz MK, Wittekind C, International Union against Cancer. *TNM classification of malignant tumours*, 7th edn. Wiley-Blackwell (2010).

FIGURE LEGENDS

Fig. 1. Characterization of IL-11$^+$ Cells in CAC Using *Il11-Egfp* Reporter Mice. **a** Protocol for induction of AOM/DSS-induced CAC in mice. *Il11-Egfp* reporter mice were intraperitoneally injected with AOM on day 0, followed by repeated DSS administration. Colorectal cancer gradually develops on ~30 days after AOM injection. Unless otherwise indicated, the following experiments used tumor and nontumor tissues collected on day 98–105 after AOM/DSS treatment. **b** Representative image of tumor and adjacent nontumor tissues in the colon of mice on day 77 after AOM injection. Colonic sections were stained with hematoxylin & eosin (H&E). Scale bar, 200 μm. **c** Prepared mRNA samples from tumor and nontumor tissues were analyzed by qPCR to determine expression of the indicated genes. Results are mean ± SE (n = 6–10 mice). **d, e** From colonic tumor tissues of wild-type or *Il11-Egfp* reporter mice, single-cell suspensions were prepared, and percentages of IL-11$^+$ cells were determined. Representative flow cytometry images are shown (**d**). Results are mean ± SE (n = 7 mice). Cells were stained with the indicated antibodies, and expression on EGFP$^+$ cells was analyzed by flow cytometry (**e**). Results are representative of four independent

958 experiments. **f** Nontumor and tumor tissue sections were stained with anti-GFP antibody.
959 Scale bars, 100 μm. **g, h** Tumor sections were stained with the indicated antibodies (red)
960 and with anti-GFP antibody (green) (n = 3 mice). Right panels show enlarged images of
961 white boxes from left panels. White arrowheads indicate merged cells. Scale bars, 100
962 μm, unless otherwise indicated. Statistical significance was determined by two-tailed
963 unpaired Student's *t*-test (**c, d**). *p < 0.05; **p < 0.01; ***p < 0.001.
964
965 **Fig. 2.** IL-11^{+} Cells Appear in Tumor Tissues in the Absence of Inflammation. **a**
966 Elevated *Il11* and *Egfp* expression in colonic tumors from *Apc*$^{min/+}$*;Il11-Egfp* reporter
967 mice. Experiments were performed using tumor and nontumor tissues from the colon of
968 20- to 24-week-old *Apc*$^{min/+}$*;Il11-Egfp* reporter mice. *Il11* and *Egfp* mRNA expression
969 was determined by qPCR. Results are mean ± SE (n = 5 mice). **b** Colonic tissue sections
970 from *Apc*$^{min/+}$;*Il11-Egfp* reporter mice were stained with H&E (upper panels) or
971 anti-GFP antibody (lower panels). Middle and right panels, respectively, show
972 enlargements of the black and red boxes from the left panels. Red arrowheads indicate
973 tumor cells. Scale bar, 100 μm. **c, d** IL-11^{+} cells express stromal cell markers and, to a

lesser extent, hematopoietic or epithelial cell markers. Colonic cells were prepared from tumors of *Apc*$^{min/+}$;*Il11-Egfp* reporter mice, stained with the indicated antibodies, and analyzed by flow cytometry. Percentages of IL-11^{+} cells were determined (**c**). Results are mean ± SE (n = 3 mice). Representative histograms show expressions of the indicated markers on EGFP^{+} cells (**d**). Results are representative of three independent experiments. **e–g** Characterization of IL-11^{+} cells by IHC. Colonic tumor sections from *Apc*$^{min/+}$;*Il11-Egfp* reporter mice were stained with the indicated antibodies (red) and anti-GFP antibody (green). White arrowheads indicate merged cells. Scale bar, 100 μm, unless otherwise indicated. Statistical significance was determined by two-tailed unpaired Student's *t*-test (**a, c**). **p < 0.01; ***p < 0.001.

Fig. 3. IL-11^{+} Cells Appear in the Colon of DSS-Treated Mice and Express Stromal Cell Marker. **a** *Il11-Egfp* reporter mice were treated with 1.5% DSS in drinking water for 5 days, followed by a change to regular water. On day 7 after DSS treatment, *Il11* and *Egfp* mRNA expression in the colon was determined by qPCR. Results are mean ± SE (n = 9 mice). **b, c** Appearance of IL-11^{+} cells in submucosal tissues of the colon of

990 *Il11-Egfp* reporter mice on post-DSS treatment day 5 (b) or day 1 (**c**). Colonic tissue
991 sections from untreated or DSS-treated *Il11-Egfp* reporter mice were H&E stained or
992 immunostained with anti-GFP antibody. Right panels show enlargements of the boxes
993 (b). Scale bar, 100 μm. **d, e** Characterization of cell surface markers on IL-11^{+} cells.
994 Colonic cells were prepared from the colon of *Il11-Egfp* reporter mice as in (**b**). We
995 determined the percentages of EGFP^{+} (IL-11^{+}) cells from the colon before and after
996 DSS treatment (**d**). Cells were stained with the indicated antibodies, and marker
997 expressions were analyzed on GFP-positive cells (**e**). Results are representative of three
998 independent experiments. **f** Representative immunostaining of IL-11^{+} cells. Colonic
999 tissue sections were prepared from *Il11-Egfp* reporter mice as in (**b**), and
1000 immunostained with the indicated antibodies and anti-GFP antibody. Results are merged
1001 images. Right panels are enlarged images from the boxes (n = 3–4 mice). White
1002 arrowheads indicate merged cells. **g** IL-11^{+} cells do not proliferate *in situ*. *Il11-Egfp*
1003 reporter mice were treated with DSS as in (**a**), and intraperitoneally administered BrdU
1004 (40 mg/kg) on day 6. On day 7, colonic sections were prepared and stained with
1005 anti-GFP and anti-BrdU antibodies. Results are representative images from three

independent experiments. Scale bars, 100 μm, unless otherwise indicated. Statistical significance was determined by two-tailed unpaired Student's *t*-test (**a**). *p < 0.05.

Fig. 4. IL-11^{+} Cells Express Genes Associated with Cell Proliferation and Tissue Repair. On day 7 after DSS treatment, cells were isolated from the colon of *Il11-Egfp* reporter mice, and IL-11^{+} cells (EGFP^{+}) were sorted by flow cytometry. We isolated mRNA from IL-11^{-} and IL-11^{+} cells, and analyzed the gene expression by microarray analysis (n = 3). **a** Heat map of microarray gene expression of IL-11^{-} and IL-11^{+} cells. Legend on right shows gene-expression color normalized by Z-score transformation. **b** Volcano plot of whole genes. Horizontal line indicates genes differentially regulated in IL-11^{+} cells compared to IL-11^{-} cells, shown in log2. Vertical line indicates p values of statistical significance, shown in −log10. Significantly upregulated and downregulated genes are indicated by red and blue dots, respectively. Several upregulated genes are plotted. **c** Gene Ontology (GO) terms that were significantly enriched in IL-11^{+} cells compared to IL-11^{-} cells. **d, e** Gene expressions were analyzed by qPCR. Results are mean ± SE (n = 4 mice). Statistical significance was determined by two-tailed unpaired

1022 Student's *t*-test (**c, d**). *p < 0.05; **p < 0.01; ***p < 0.001; ns, not significant.

1023

1024 **Fig. 5.** The MEK/ERK Pathway is Involved in *Il11* Upregulation in Tumor Tissues. **a, b**

1025 Wild-type mice were treated with DSS with or without NAC (**a**) or Abx (**b**). Colonic

1026 cells were prepared and stained with CellRox-green, and ROS accumulation was

1027 analyzed by flow cytometry. Left panels show representative histograms of ROS levels

1028 in colonic cells. Right panels show percentages of CellRox-green-positive cells of an

1029 individual mouse. Results are mean ± SE (n = 3–4 mice). **c** Wild-type mice were treated

1030 as in A. Colonic expressions of *16S rRNA, Hmox1,* and *Il11* mRNA were determined by

1031 qPCR. Results are mean ± SE (n = 11). **d** Abx blocked *Il11* mRNA upregulation in the

1032 colon of DSS-treated mice. Wild-type mice were untreated or treated with DSS in the

1033 absence or presence of Abx. On day 7 after DSS treatment, qPCR was performed to

1034 determine the expression of bacterial *16S rRNA* and *Il11* mRNA in the colon. Results

1035 are mean ± SE (n = 10). **e, f** Trametinib inhibits ERK phosphorylation and *Il11* mRNA

1036 expression in the colon of DSS-treated mice. Wild-type mice were treated with DSS in

1037 the absence or presence of trametinib, and then colonic sections were prepared and

1038 stained with anti-pERK antibody (**e**). Scale bars, 100 μm. *Il11* mRNA expression was
1039 determined by qPCR (**f**). Results are mean ± SE (n = 13–14). **g** NAC inhibits ERK
1040 phosphorylation in the colon of DSS-treated mice. Wild-type mice were treated with
1041 DSS in the absence or presence of NAC in the drinking water for 5 days. Colonic
1042 sections were stained with anti-pERK antibody. Results are representative of three
1043 independent experiments. Scale bar, 100 μm. **h** *Tgfbs* expression in the colon of
1044 DSS-treated wild-type mice. Wild-type mice were treated with DSS as in Fig. 4a. On
1045 day 7 after DSS treatment, qPCR was performed to determine *Tgfb1, Tgfb2*, and *Tgfb3*
1046 mRNA expression in the colon. Results are mean ± SE (n = 8–10 mice). **i** Treatment
1047 with anti-TGFβ antibody does not downregulate *Il11* mRNA expression in the colon of
1048 DSS-treated mice. Mice were intraperitoneally administered 100 μg anti-TGFβ
1049 antibody on days 2 and 4 after DSS administration, and sacrificed on day 5. *Il11* mRNA
1050 expression was determined by qPCR. Results are mean ± SE (n = 11–16 mice). **j**
1051 Schema of administration of various inhibitors in AOM/DSS-treated mice. Mice were
1052 treated with Abx for 8 weeks, NAC for 4 weeks, trametinib at −6 and −30 hours, or
1053 anti-TGFβ antibody on day −1, −3, −5 (just before sacrifice). **k–m, o** Mice were treated

as in Figure 1A, and then treated with Abx (**k**) (n = 7–9 mice), NAC (**l**) (n = 7–11 mice), trametinib (**m**) (n = 10–12 mice), or anti-TGFβ antibody (n = 6–7 mice) (**o**) as in (**j**). On day 98–105 after AOM injection, mRNA was extracted from tumor and non-tumor tissues, and *Il11* expression was determined by qPCR. Results are mean ± SE. **n** Mice were treated as in Fig. 1a. *Tgfb1*, *Tgfb2,* and *Tgfb3* expressions in tumor and nontumor tissues were determined by qPCR. Results are mean ± SE (n = 7 mice). Statistical significance was determined using the unpaired two-tailed Student's *t*-test (**c, h**), Mann-Whitney U test (**f, i**), two-way ANOVA with Bonferroni's test (**d, k, l, m, o**), or one-way ANOVA with Tukey's post-hoc test (**a, b**). *p < 0.05; **p < 0.01; ***p < 0.001; ns, not significant.

Fig. 6 IL-11 Preferentially Induces Signals to Fibroblasts. **a** Relative expressions of *Il11ra1*, *Il22ra1*, and *Il6st* in colonic epithelial organoids and colonic fibroblasts. Colonic epithelial organoids and fibroblasts were established from wild-type mice as described in the methods. Expressions of the indicated genes were determined by qPCR. Results are mean ± sd of triplicate samples and representative of two independent

experiments. **b** Colonic epithelial organoids and fibroblasts were unstimulated or stimulated for 30 min with IL-11 (10 or 100 ng/mL) or IL-22 (10 or 100 ng/mL). Total STAT3 and phosphorylated STAT3 (pSTAT3) were analyzed by Western blotting. STAT3 and pSTAT3 signaling intensities were calculated by Fiji, and the relative ratio of pSTAT3/STAT3 is shown. Results are representative of two independent experiments. **c** Administration of IL-11R agonist induces expression of the genes expressed in IL-11$^+$ cells. We injected 8-week-old wild-type mice with 10 μg IL-11R agonist. At 3 hours after injection, mRNA was isolated from the colon, and gene expressions were analyzed by microarray analysis (n = 2 for untreated samples; n = 3 for injected samples). Heat map of microarray gene expression in the colon of untreated and treated mice (**c**). Legend on the right shows gene-expression color normalized by Z-score transformation. **d** Volcano plot of whole genes. Horizontal line indicates differentially regulated genes in the colon after IL-11R agonist injection compared to before injection, shown in log2. Vertical line indicates p values of statistical significance, shown in −log10. Significantly upregulated genes are indicated by red dots. Several upregulated genes are plotted. **e** Venn diagram of genes elevated in IL-11$^+$ IAFs compared to IL-11$^-$ cells, and genes

1086 elevated in the colon with IL-11R agonist treatment compared to untreated colon.
1087 Overlapping area includes 18 genes. Statistical significance was determined by
1088 two-tailed unpaired Student's *t*-test (**a**). *p < 0.05; **p < 0.01; ****p < 0.0001.
1089
1090 **Fig. 7.** IL-11 Expression is Correlated with Progression of Human Cancers. **a**
1091 Specificity of anti-IL-11 antibody used in the study. MDA-MB-231 cells were treated
1092 with control or three different siRNAs against human *Il11*, and IL-11 expression in cell
1093 lysates was analyzed by Western blotting with anti-IL-11 and anti-tubulin antibodies.
1094 Results are representative of two independent experiments. **b-d** Adenomas (n = 10),
1095 early (n = 10) and advanced (n = 10) colorectal cancers were stained with anti-IL-11
1096 antibody (**b**). Representative staining of respective tumors and adjacent normal tissues.
1097 Scale bars, 100 μm. Areas (**c**) and intensities (**d**) of IL-11^{+} signals were calculated as in
1098 the methods. Results are mean ± SE. **e** Tissues of advanced colorectal cancers were
1099 stained with anti-vimentin, anti-CD45, or anti-E-cadherin antibodies along with
1100 anti-IL-11 antibody (n = 3). Right panels are enlarged images of the white box in the
1101 left panels. Signaling intensities stained with the indicated antibodies on the white

1102 arrows were calculated and plotted in the right panels. Scale bars, 100 μm. Statistical

1103 significance was determined by Mann-Whitney U test (**c, d**). **p < 0.01; ns, not

1104 significant.

1105

1106

NishinaFig1

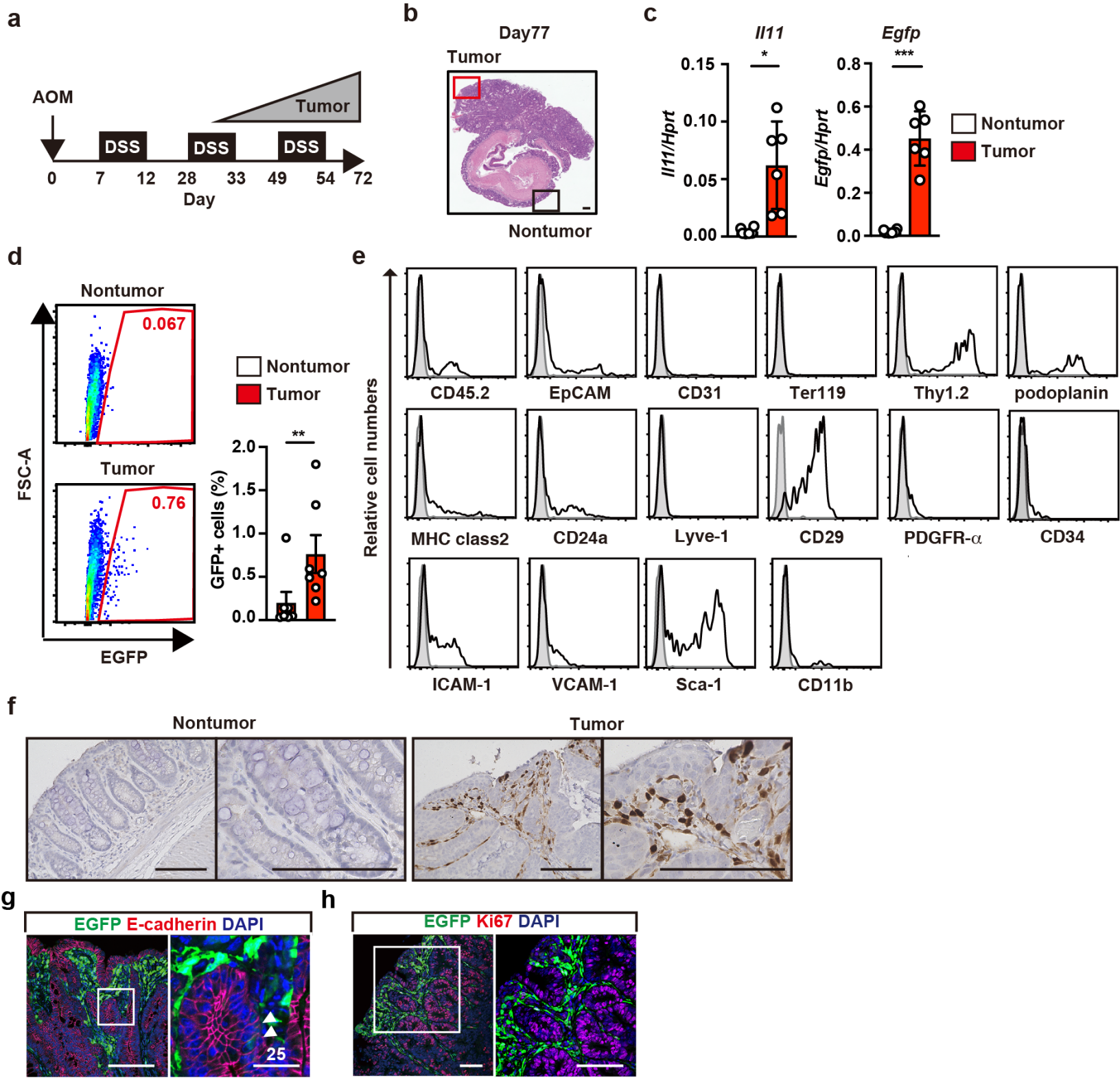

NishinaFig2

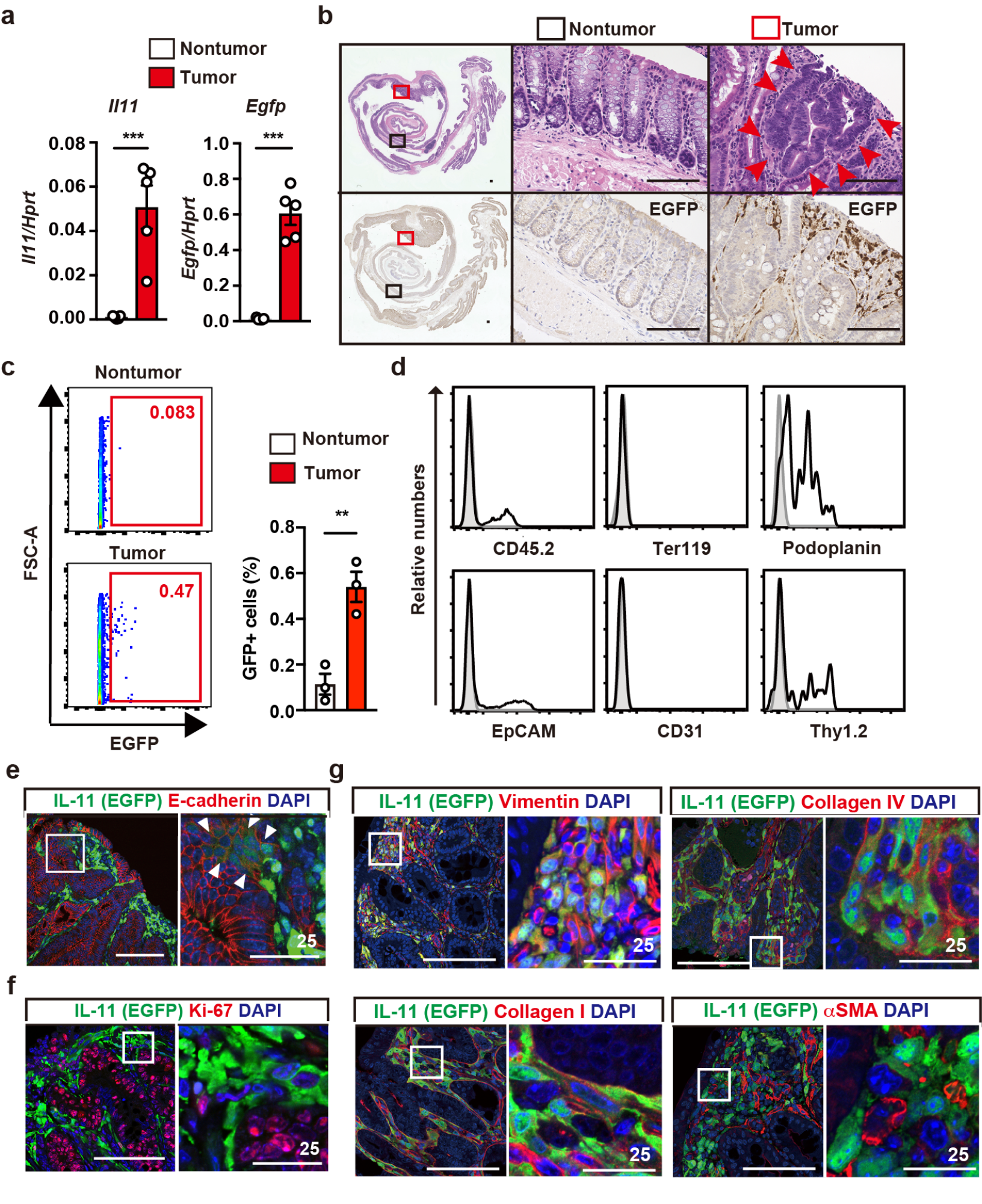

Nishina Fig3

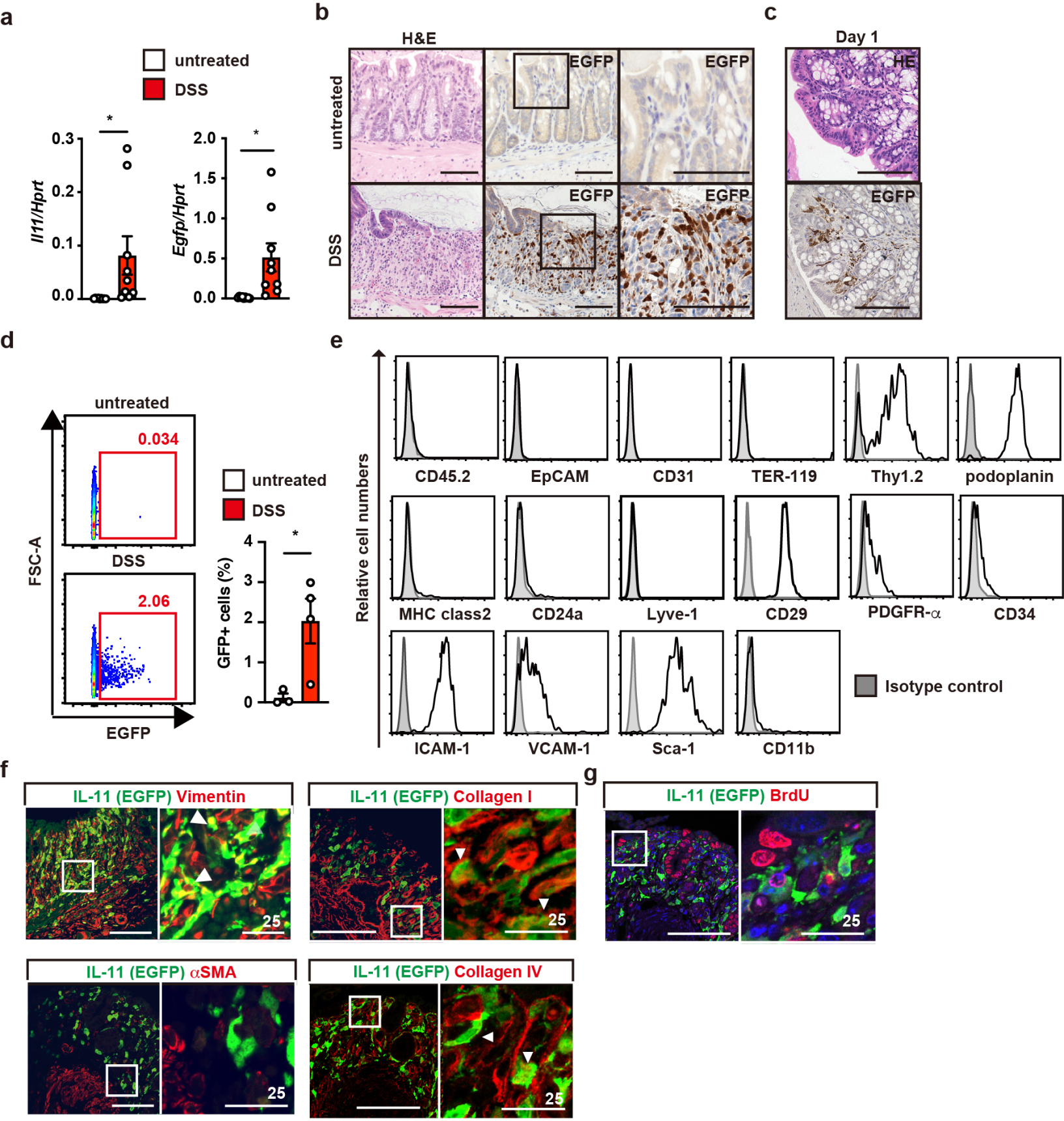

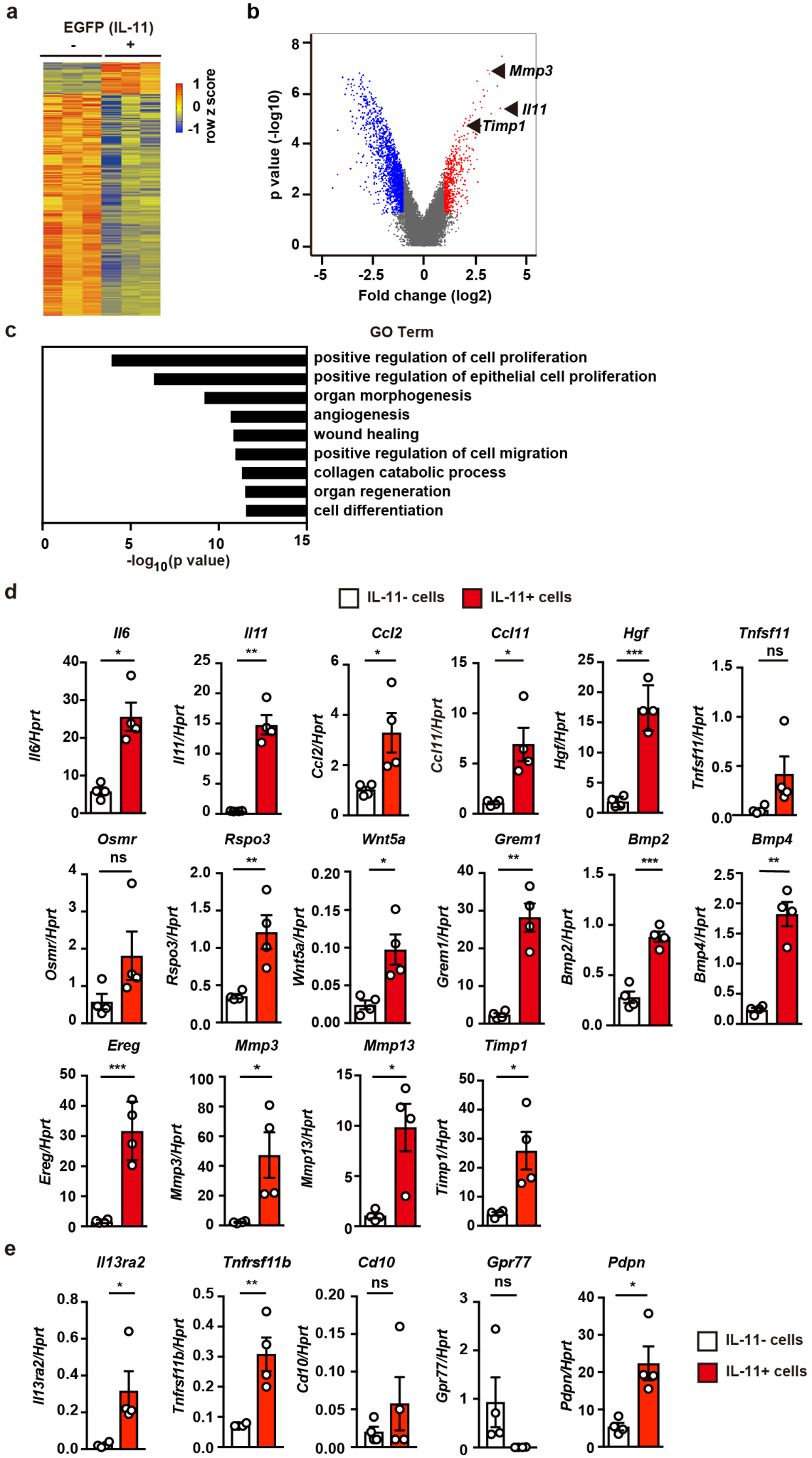

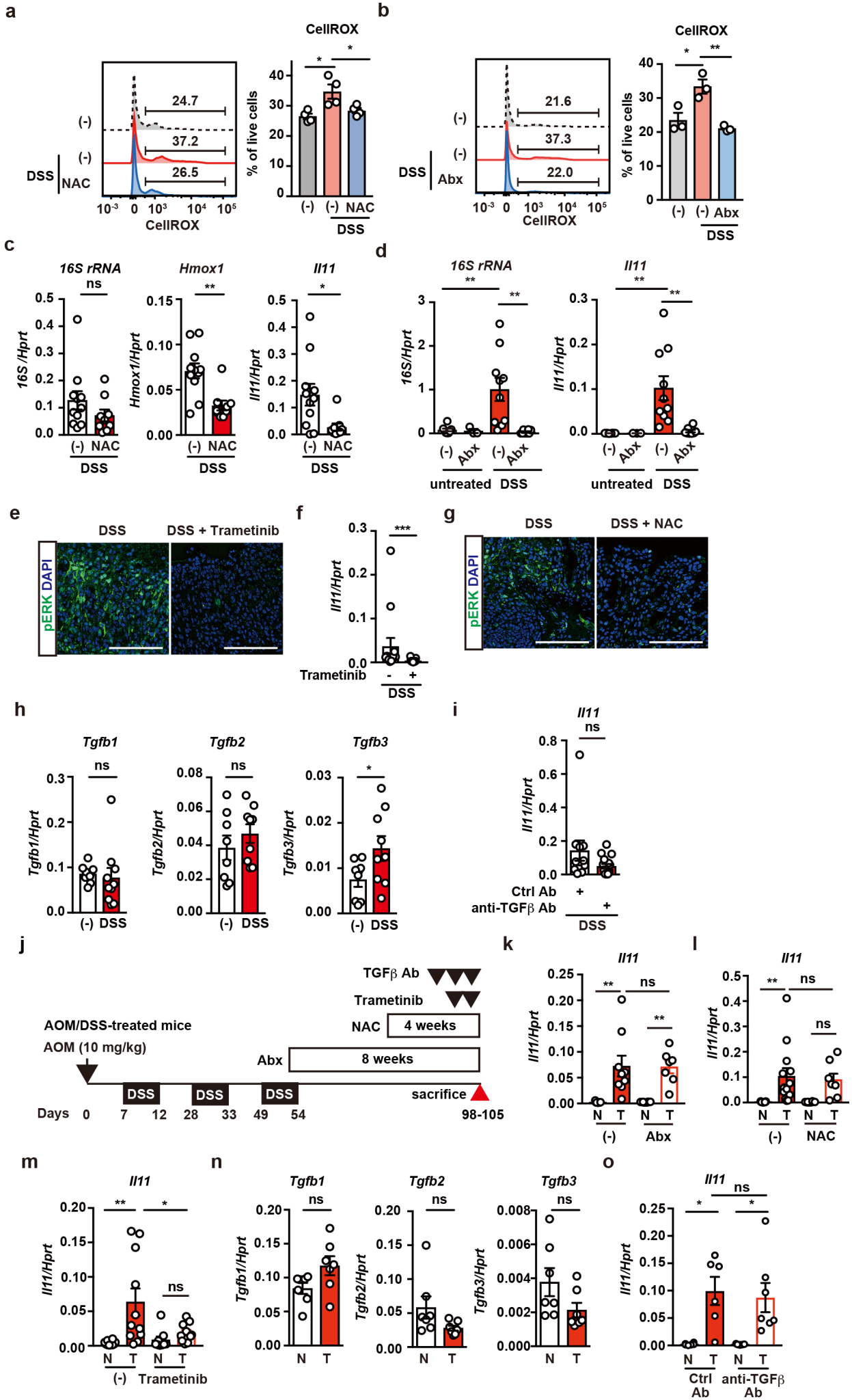

a

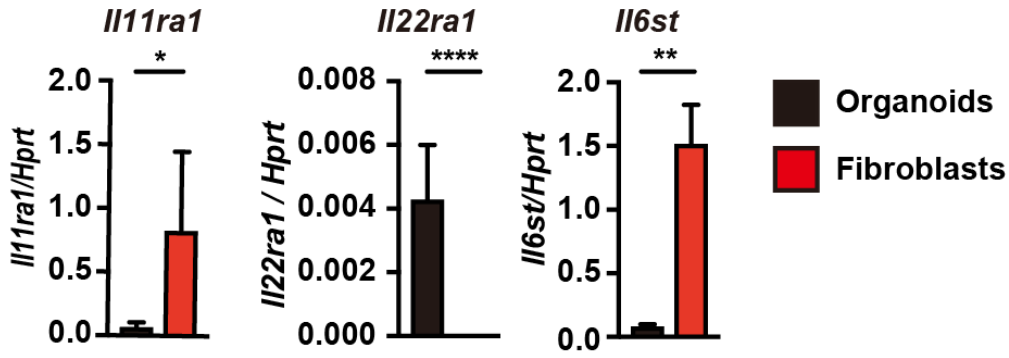

b

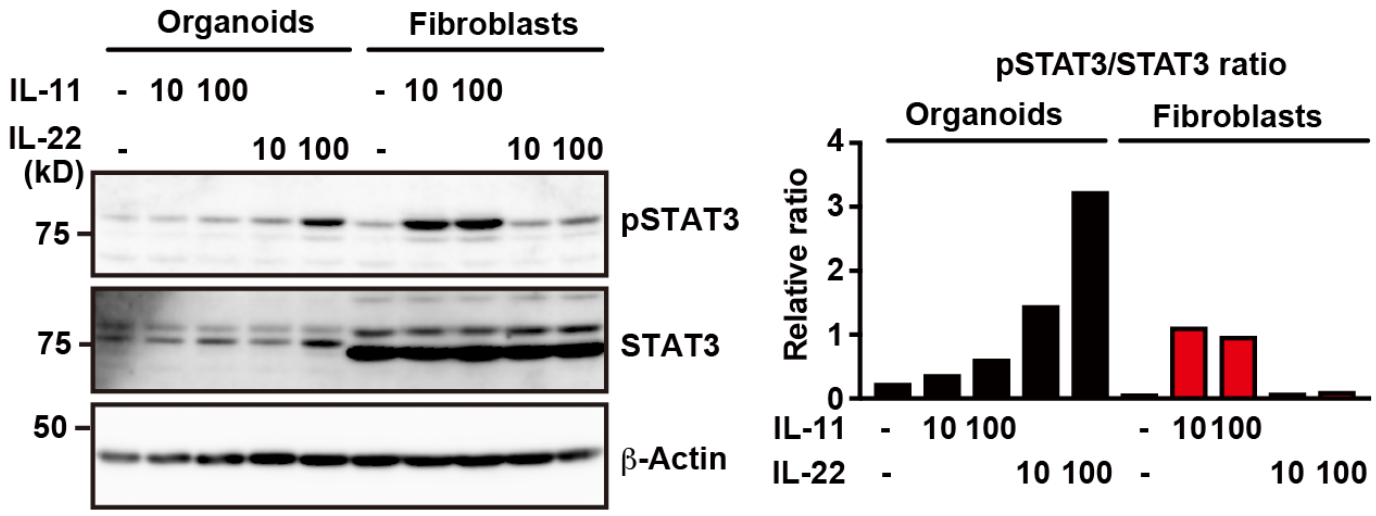

c

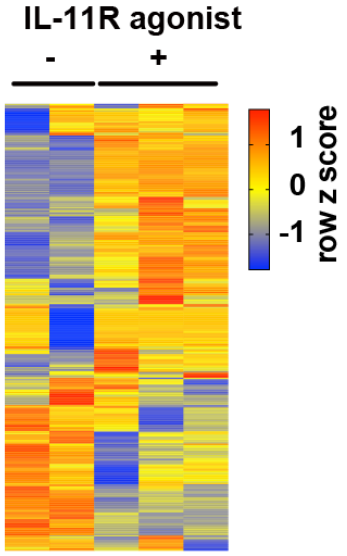

d

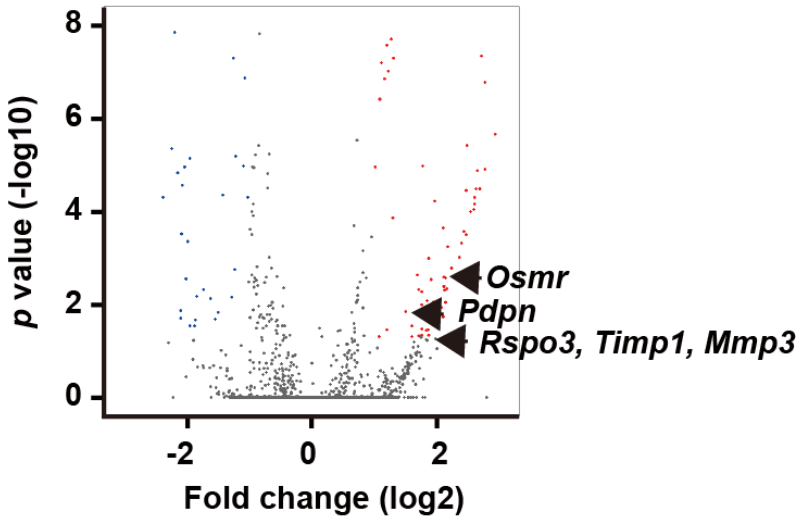

e

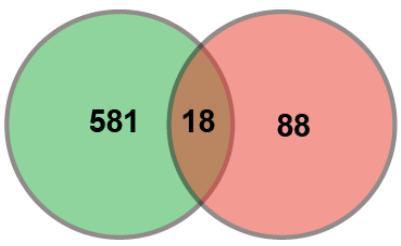

Mmp10	*Hgf*
Adamdec1	*Tspan4*
Nbl1	*Timp1*
Mmp3	*Cxcl5*
Osmr	*Chrdl2*
Rasl11a	*Gem*
Serpina3m	*Ifitm1*
Iigp1	*Pdpn*
Ccl7	*Rspo3*

NishinaFig7

a

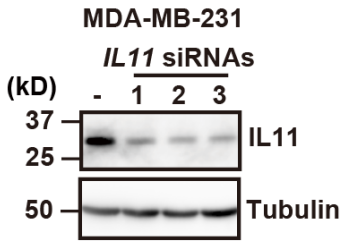

b

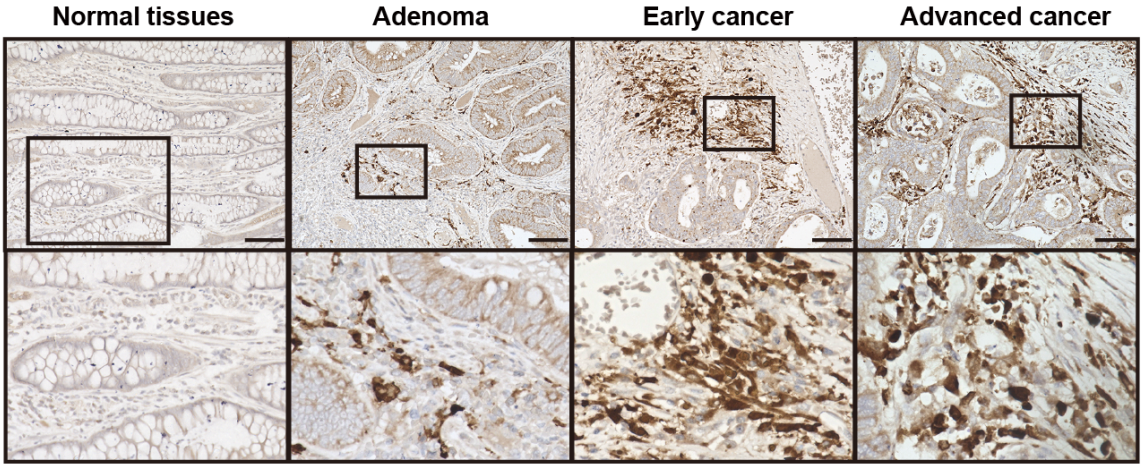

c

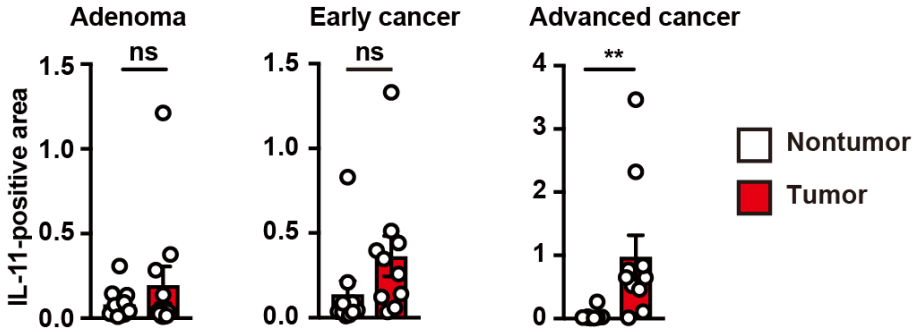

d

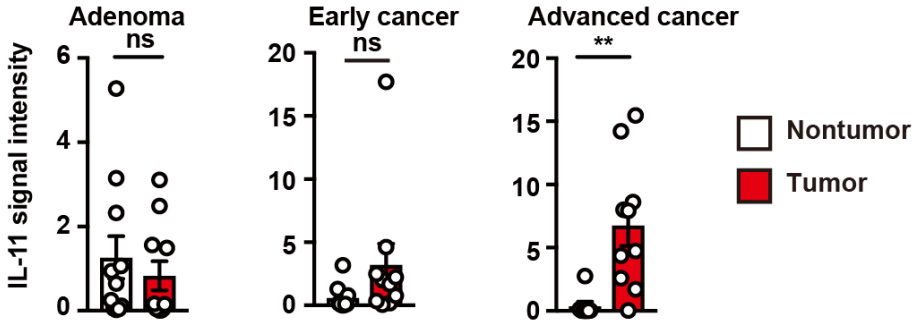

e